

EVOL (Project n°249696)
FINAL REPORT

PARTNERS: CNRS, JRC-ITU, TUD, HZDR, KIT, POLITO, AD, EVM, BME, UOXF-DJ, INOPRO, PSUD

OBSERVER: POLIMI, PSI

COLLABORATION: ROSATOM

SUMMARY

A.I- DESCRIPTION OF THE MSFR CONCEPT

A.I.1- Concept overview

A.I.2- Systems description of the MSFR fuel circuit

A.I.3- Chemical properties and core geometry

A.II- OPTIMISATION OF CORE GEOMETRY

A.II.1- Neutronic benchmark

A.II.2- Alternative MSFR spherical core shape design

A.III- RECOMMENDATIONS FOR AN MSFR DEMONSTRATOR PRE-CONCEPTUAL DESIGN

A.III.1- Power demonstrator

A.III.2- From a demonstrator to a modular reactor

A.IV- MOLTEN SALT REACTOR SAFETY ANALYSIS

A.V- CONCLUSIONS AND PERSPECTIVES

B.I- FUEL CHEMISTRY

B.I.1- Selection of a fuel salt composition

B.I.2- Physico-chemical properties of the fuel salt

B.I.3- Conclusion

B.II- RECOMMENDATIONS OF A REPROCESSING SCHEME

B.II.1- Definition of the reprocessing scheme

B.II.2- Chemical and physical state of the elements during the reprocessing

B.II.3- Redox potential control of the salt

C.I- STRUCTURAL MATERIALS FOR MSFR CONCEPT

C.I.1- Metallurgy of NiWCr alloys

C.I.2- Mechanical properties of NiWCr alloys

C.I.3- Corrosion of NiWCr alloys

C.I.4- Conclusion and recommendations

D- TRAINING AND DISSEMINATION ACTIVITIES

A.I- DESCRIPTION OF THE MSFR CONCEPT

Molten Salt Reactors (MSRs) have seen a marked resurgence of interest over the past decades, highlighted by their inclusion as one of the six candidate reactors of the Generation IV advanced nuclear power systems with expected remarkable advantages in safety, economics, sustainability, and proliferation resistance.

Starting from the Oak-Ridge National Laboratory (ORNL) Molten Salt Reactor Experiment (MSRE) and Molten Salt Breeder Reactor project (MSBR)¹, based on extensive parametric studying, an innovative concept called Molten Salt Fast Reactor (MSFR)^{2 3 4 5 6 7 8 9}. This concept results from extensive parametric studies in which various core arrangements, reprocessing performances and salt compositions were investigated with a view to the deployment of a thorium based reactor fleet on a worldwide scale. The primary feature of the MSFR concept versus that of other older MSR designs is the removal of the graphite moderator from the core (graphite-free core), resulting in a breeder reactor with a fast neutron spectrum and operated in the Thorium fuel cycle as described below. The MSFR has been recognized as a long term alternative to solid fuelled fast neutron systems with a unique potential (excellent safety coefficients, smaller fissile inventory, no need for criticality reserve, simplified fuel cycle...) and has thus been officially selected for further studies by the Generation IV International Forum since 2008¹⁰.

A.I.1- Concept overview

The reference MSFR is a 3000 MWth reactor with a fast neutron spectrum and based on the Thorium fuel cycle as previously mentioned. In the MSFR, the liquid fuel processing is an integral part of the reactor where a small sample of the molten salt is set aside to be processed for fission product removal and then returned to the reactor. This is fundamentally different from a solid-fuelled reactor where separate facilities produce the solid fuel and process the Spent Nuclear Fuel. The MSFR can be operated with widely varying fuel compositions thanks to its on-line fuel control and flexible fuel processing: its initial fissile load may comprise ²³³U, ²³⁵U enriched (between 5% and 30%) natural uranium, or the transuranic (TRU) elements currently produced by PWRs.

In the MSFR concept, the nuclear fission reactions take place within the flowing fuel salt in the cavity where a critical mass is attained. The core cavity can be decomposed on three free volumes: the active core, the upper extraction volume and the lower injection volume. The salt's thermal-hydraulic behavior is closely coupled to its neutronic behavior, because the salt's circulating time (4s) and the lifetime of the precursors of delayed neutrons (around 10s) are of the same order of magnitude. A sketch of the reactor layout is presented in Figure 1.

¹ Weinberg, A. M., Collection of papers on the molten salt reactor experiment. Nuc. Appl. Technol, Vol. 8. 1970.

² S. Delpech et al, J. of Fluorine Chemistry, 130 (2009) 11

³ Nuttin A, Heuer D., et al., "Potential of Thorium Molten Salt Reactors", Prog. in Nucl. En., 46, 77-99 (2005)

⁴ Mathieu L., Heuer D., et al., "The Thorium Molten Salt Reactor: Moving on from the MSBR", Prog in NuclEng, 48, 664-679 (2006)

⁵ Mathieu L., Heuer D., Merle-Lucotte E., et al., "Possible Configurations for the Thorium Molten Salt Reactor and Advantages of the Fast Non-Moderated Version", Nucl.Sc. and Eng., 161, 78-89 (2009).

⁶ Forsberg C.W. et al., "Liquid Salt Applications and Molten Salt Reactors", Revue Générale du Nucléaire N° 4/2007, 63 (2007)

⁷ Merle-Lucotte E., Heuer D. et al., "Introduction of the Physics of Molten Salt Reactor", Materials Issues for Generation IV Systems, NATO Science for Peace and Security Series - B, Editions Springer, 501-521 (2008)

⁸ Merle-Lucotte E., Heuer D. et al., "Minimizing the Fissile Inventory of the Molten Salt Fast Reactor", Proceedings of the Advances in Nuclear Fuel Management IV (ANFM 2009), Hilton Head Island, USA -2009)

⁹ Merle-Lucotte E., Heuer D. et al., "Optimizing the Burning Efficiency and the Deployment Capacities of the Molten Salt Fast Reactor", Proceedings of the International Conference Global 2009 - The Nuclear Fuel Cycle: Sustainable Options & Industrial Perspectives, Paper 9149, Paris, France (2009)

¹⁰ Renault C. et al., "The Molten Salt Reactor (MSR) in Generation IV: Overview and Perspectives", <http://www.gen-4.org/GIF/About/documents/30-Session2-8-Renault.pdf>, Proceedings of the GIF Symposium 2009, Paris, France (2009)

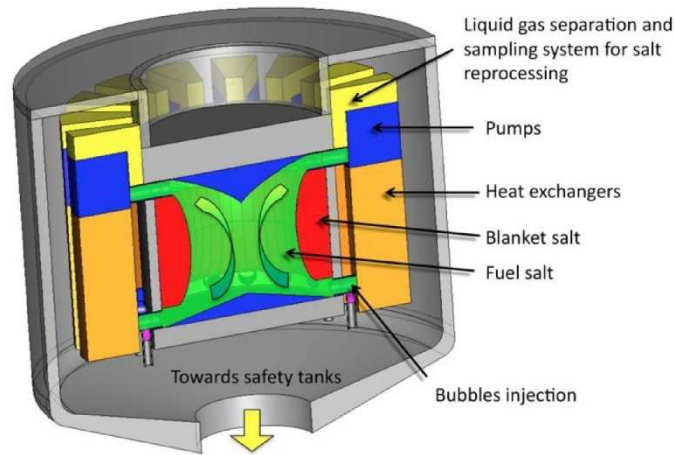


Figure 1: Conceptual design of the MSFR

Optimization studies have been performed prior the beginning of the EVOL project, relying on neutronic considerations (feedback coefficients and breeding capacities), material damages and heat evacuation efficiency, and resulting in MSFR configurations with a total fuel salt volume of 18 m³, half of the salt (9 m³) located in the core and half in the external circuits as explained above. Based on these preliminary studies and for the purpose of the current analysis the core cavity was assumed to have a cylindrical shape with a height to diameter ratio (h/d) equal one (to minimize the neutron leaks and thus improves the breeding ratio). A more complete description of the design was given in the deliverable 2.2. More details on the whole system have been given in the deliverable 2.8.

A.1.2- Systems description of the MSFR fuel circuit

In order to initiate the work and the discussions on possible ranges for the reactor parameters, basic drawings have been developed from the preliminary conceptual design. Figure 2.2 illustrates one of the possible geometrical configurations. During normal operation, the fuel salt circulates in the core and in 16 external modules, so called fuel loops. Each of them contains a pump, a heat exchanger and a bubbling system (external modules). The time circulation of the fuel salt is of the order of a few seconds, depending on the specific core power and the salt temperature rise (ΔT) in the core.

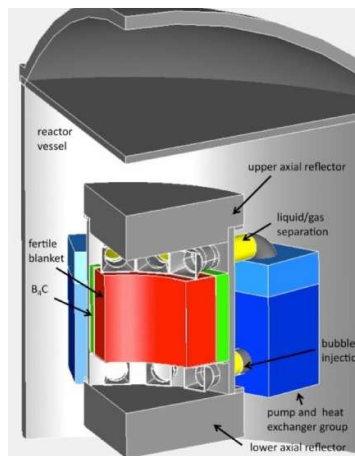


Figure 2: Example of a 3-D layout for the Molten Salt Fast Reactor (MSFR)

Core: The core active region is defined as the salt volume where most nuclear fissions take place. It includes the flowing salt in the central cavity, the injection zone (in the bottom part of the core) and

the extraction zone (top of the core). In the MSFR core there is no solid moderator or any internal support structure except for the wall materials. As previously mentioned, the reference concept is designed for a nominal power of 3 GWth, with a salt temperature rise preliminary fixed at $\Delta T = 100$ K. The operating temperatures chosen in the initial simulations were 650°C (inlet temperature) and 750°C (outlet temperature). The lower limit due to the salt's melting point (565°C) while the upper limit is imposed by the structural materials performance (limit around 800°C due to materials constraints). The core working parameters were defined after performing various parametric studies seeking for low neutron losses, low reflector irradiation and minimal fissile inventory, while maintaining a fuel salt volume in the heat exchangers large enough to ensure that salt cooling by $\Delta T = -100$ K is feasible. The resulting core shape is roughly a cylinder, with 1/2 of the entire salt volume inside the core, the rest being located in the external fuel loops. This core geometry has to be further optimized to guaranty a stable flow in the core.

Fuel Salt: The choice of the fuel salt composition relies on several parametric reactor studies (chemical and neutronic considerations, burning capabilities, safety coefficients, and deployment capabilities). The optimal fuel salt composition is a binary fluoride salt, composed of LiF enriched in ^7Li to 99.995 % and a heavy nuclei (HN) mixture initially composed of fertile thorium and fissile matter. The salt composition definition was a key point of the project. That will be detailed further. This salt composition leads to a fast neutron spectrum in the core. With a fusion temperature of 565°C, the mean operating temperature has been chosen at around 700°C (see above). The fission products created during operation can be soluble or insoluble in the salt. To maintain the physico-chemical and neutronic characteristics of the salt, it is necessary to clean the salt, i.e., to extract the fission products. It is important to stress that due to the fast neutron spectrum of the MSFR the impact of the fission products on the neutronic economy is relatively small and thus the control of the physico-chemical properties is clearly the main aim of the reprocessing unit. The temperature of the salt depends strongly on the operation of the pumps and the cooling in the heat exchangers.

Upper and Lower Reflectors: The lower and upper walls of the core are neutronic reflectors. A NiCrW hastelloy has been selected as a structural material candidate for the reflectors walls (and for all other internal walls in contact with the fuel salt). The upper reflector is submitted to mechanical, thermal and radiation constraints. The combination of high temperature and high radiation levels seem to be the biggest challenge for the proposed alloy so that the surface of the upper reflector may require a thermal protection. Due to the significant lower inlet temperature, the lower reflector is under reduced thermal stress. Its specificity is to be coupled to the draining system. Optimized shapes of these reflectors will be studied to insure the most stable thermal flow in the core.

Fertile Blanket: This component serves as radial reflector and as a neutron shield to protect the external components of the fuel loops (pipes, heat exchangers). In addition to this protection function, the fertile blanket is used to improve the breeding capabilities of the reactor. The walls of the blanket containment are made of a Ni-based alloy for corrosion resistance and have an external layer of B_4C on the outer wall to further reinforce the neutronic shielding. The salt in the blanket is of the same type as the one in the core but with 22.5 mol% of Th and without any initial fissile material. Since the thorium present in the fertile salt is exposed to the core neutron flux, it will generate the ^{233}U fissile element. A small fraction of the ^{233}U produced in the blanket will fission so that fission products are produced in the blanket and will need to be extracted. In addition, the power arising from the ^{233}U fissions (13MW) and from the captures on thorium (24MW) will heat-up the fertile salt in the blanket. It has been found that this heat cannot be evacuated through the blanket walls by a natural convection mechanism of the fertile salt. Therefore a fertile blanket external cooling system will be necessary. If breeding is not required, the MSFR design could be simplified by replacing the fertile blanket by an inert reflector, identical to the axial reflectors. Optimized shapes of the fertile blanket may also be studied to improve the thermal flow in the core.

Heat Exchanger (x16): Each heat exchanger (HX) unit has to extract about 187 MW during normal operation. The HX design is challenging since a very compact design is needed (to reduce the volume of the fuel salt outside the core) but on the other hand the maximum compactness achievable has to be limited by considerations on the HX pressure drop, the maximum velocity allowed for the salt (erosion) and the thermodynamic properties of the working fluids. A preliminary design has been developed based using a plate heat exchanger type which allow a reasonable compromise between compactness (exchange surface) and pressure drop. This preliminary design is adequate for the purpose of the current benchmarks but will require further studies (in particular related to the geometry, materials and fabrication) to allow for a better optimization. The design of this component impacts the heating ΔT in the core when both reactor power and total fuel volume fixed.

Pump (x16): The salt is circulating in the reactor by sixteen pumps located in each of the fuel loops. The fuel salt flow rate is about $0.28 \text{ m}^3/\text{s}$ to guaranty an adequate temperature rise in the core for the current core power level. The power of the pumps has an impact on the circulation time of the salt and thus on the heating in the core.

Pipes: The piping system allows the circulation of salt between the core and the HX and pumps. The pipes are sized (diameter and length) according to two main constraints: reduce the fuel salt volume outside the core and limit the maximum salt speed in the pipes (to avoid erosion). Varying the pipes diameter impacts the circulation period of the fuel salt in the whole system, and thus its heating in the core if the power is fixed. Other considerations that will have to be analyzed in the future include optimization of the pressure drop, thermal fatigue (in particular in the upper pipes), pipe vibration, welding, seismic behavior, access for inspection, thermal shielding.

Reactor Vessel: The core and the reactor systems (components of fuel loops such as pipes, pumps, HX, etc.) described before are contained inside a reactor vessel which is filled with an inert gas (argon). As in the original experimental reactor MSRE, the inert gas has a double function: it is used to cool down the reactor components by maintaining the gas temperature at about around 400°C ; and it allows for sampling to early detect a possible salt leak. Note fixing the gas temperature at 400°C will guarantee that in the event of a small fuel salt leak, the salt should solidify since its melting temperature is equal to 565°C . The reactor vessel parameters (geometrical and material) do not directly impact the core performance (and thus are not needed for the optimization) but will be necessary for the safety analysis.

A.I.3- Chemical properties and core geometry

Physicochemical properties of the molten salts used in the MSFR

New measurements of the physico-chemical properties of fluoride salts have been performed in the frame of EVOL, MARS and ISTC #3749 projects, the properties for a salt of LiF (78 mol%)- ThF_4 (22 mol%) are listed in Table 1. The third column summarizes the values used for simulation in the benchmark, at a mean temperature of 700°C (halfway between the low and the high operating temperatures). During reactor operation, fission products and new heavy nuclei are produced in the salt up to some mole% only, we have considered that they do not impact the salt physicochemical properties. The same data are used in the simulations for the fertile salt.

Table 1: Physicochemical properties used for the fuel and fertile salt in the benchmark, measured for the salt 78%mol LiF-22%mol ThF₄¹¹

	Formula	Value at 700°C	Validity Range, °C
Density ρ (g/cm ³)	$4.094 - 8.82 \cdot 10^{-4} (T_{(K)} - 1008)$	4.1249	[620-850]
Kinematic Viscosity ν (m ² /s)	$5.54 \cdot 10^{-8} \exp\{3689/T_{(K)}\}$	$2.46 \cdot 10^{-6}$	[625-846]
Dynamic viscosity μ (Pa.s)	$\rho_{(g/cm^3)} \cdot 5.54 \cdot 10^{-5} \exp\{3689/T_{(K)}\}$	$10.1 \cdot 10^{-3}$	[625-846]
Thermal Conductivity λ (W/m/K)	$0.928 + 8.397 \cdot 10^{-5} \cdot T_{(K)}$	1.0097	[618-747]
Calorific capacity C_p (J/kg/K)	$(-1.111 + 0.00278 \cdot T_{(K)}) \cdot 10^3$	1594	[594-634] ^a

Structural materials

The reflectors are made of a Ni-based alloy. The density of the Ni-based alloy, whose composition is detailed in Table 2, is equal to 10. This material will not be submitted to a high neutron flux. Hence the choice of its composition is not too constrained.

Table 2: Composition (at%) of the Ni-based alloy considered for the simulation of the structural materials of the core

Ni	W	Cr	Mo	Fe	Ti	C	Mn	Si	Al	B	P	S
79.432	9.976	8.014	0.736	0.632	0.295	0.294	0.257	0.252	0.052	0.033	0.023	0.004

Concerning the neutronic protection, we have considered the composition of natural boron: 19.8% of 10B and 80.2% of 11B. The B₄C density is equal to 2.52016 (data used in SIMMER code, provided by KIT).

Geometry used in the benchmark

As shown in Figure 3, the core is a single cylinder (the diameter being equal to the height) where the nuclear reactions occur within the flowing fuel salt. The core is composed of three volumes: the active core, the upper plenum and the lower plenum. The fuel salt considered in the simulations is a binary salt, LiF - (Heavy Nuclei)F₄, whose (HN)F₄ proportion is set at 22.5 mole % (eutectic point), corresponding to a melting temperature of 565°C. The choice of this fuel salt composition relies on many systematic studies (influence of the chemical reprocessing on the neutronic behavior, burning capabilities, deterministic safety evaluation and deployment capabilities). This salt composition leads to a fast neutron spectrum in the core.

As previously mentioned, the radial reflector is a fertile blanket (50 cm thick) filled with 7.3 m³ of a fertile salt LiF-ThF₄ with molar 22.5% of ²³²Th. This fertile blanket improves the global breeding ratio of the reactor thanks to a ²³³U extraction in an around six months period, i.e. 100% of the ²³³U produced in the blanket is extracted in 192 days (40 liters per day as shown in the lower part of Fig 3). This fertile blanket is surrounded by a 20cm thick neutronic protection of B₄C which absorbs the remaining neutrons and protects the heat exchangers. The thickness of this B₄C protection has been determined so that the neutron flux arriving from the core through it is negligible compared to the flux of delayed neutrons emitted in the heat exchangers.

¹¹ Ignatiev V., Feynberg O., Merzlyakov A. et al., "Progress in Development of MOSART Concept with Th Support", Proceedings of ICAPP 2012, Paper 12394 Chicago, USA(2012)

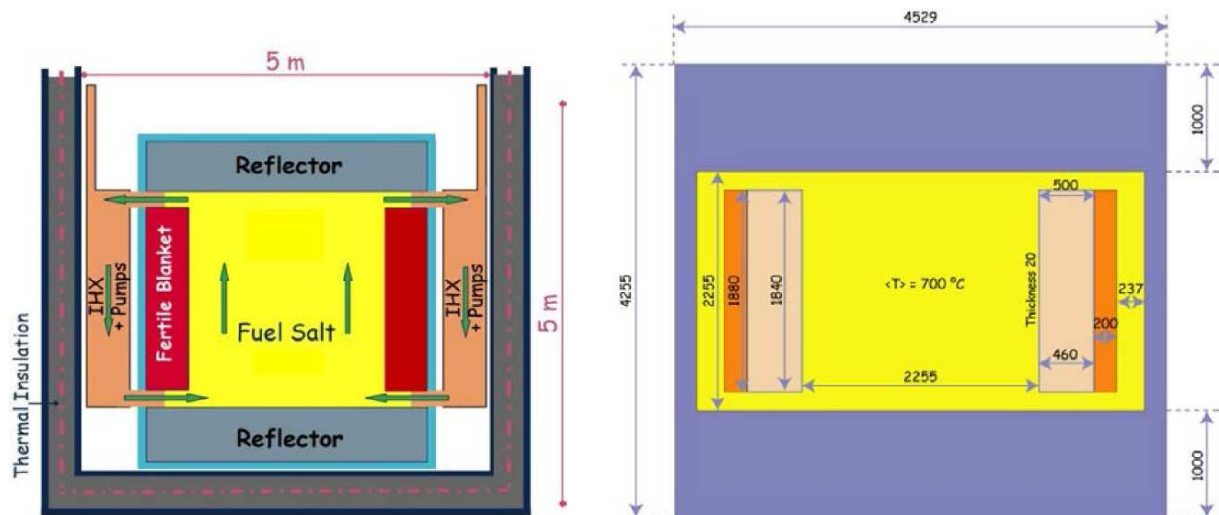


Figure 3 (Left): Simplified to scale vertical scheme of the MSFR system including the core, blanket and fuel heat exchangers (IHX) – (Right): Model of the core as used for the neutronic simulations (dimensions given in mm) with the fuel salt (yellow), the fertile salt (pink), the B_4C protection (orange) and the reflectors and 20mm thick walls in Ni-based alloy (blue)

Table 3: Characteristics of the MSFR simulated on the neutronic benchmark

Thermal power (MWth)	3000				
Electric power (MWe)	1500				
Fuel Molten salt initial composition (mol%)	LiF-ThF ₄ - ²³³ UF ₄ or LiF-ThF ₄ -(Pu-MA)F ₃ with 77.5 % LiF				
Fertile Blanket Molten salt initial composition (mole %)	LiF-ThF ₄ (77.5%-22.5%)				
Melting point (°C)	565				
Input/output operating temperature (°C)	650-750				
Initial inventory (kg)	²³³ U-started MSFR		TRU-started MSFR		
	Th	²³³ U	Th	Actinide	
	38 300	5 060	30 600	Pu	11 200
				Np	800
				Am	680
				Cm	115
Density (g/cm ³)	4.1249				
Dilatation coefficient (g.cm ⁻³ /°C) [Ignatiev et al., 2012]	8.82 10 ⁻⁴				
Core dimensions (m)	Radius: 1.1275 Height: 2.255				
Fuel Salt Volume (m ³)	18 9 out of the core 9 in the core				
Blanket Salt Volume (m ³)	7.3				
Total fuel salt cycle in the system	4.0 s				

The radial blanket geometry is an angular section toron of 188 cm high and 50 cm thick. The 2 cm thick walls are made of Ni-based alloy (see composition in Table 2). A single volume of fertile salt is considered, homogenous and cooled to a mean temperature of 650°C. A temperature variation of the fertile salt of around 30 °C between the bottom and the top of the fertile blanket may be introduced to check its low impact on the reactor evolution.

Fuel salt initial composition

The core contains a fluoride fuel salt, composed of 77.5 molar % of LiF enriched in ^7Li (99.995 at%) and 22.5 molar % of heavy nuclei (HN) which the fissile element. This HN fraction is kept constant during reactor evolution, the produced FPs replacing an equivalent proportion of the lithium. The neutronic benchmark focuses on the ^{233}U -started and the TRU-started MSFR

^{233}U -started MSFR

As detailed in Table 3, the initial fuel salt is composed in this case of $\text{LiF-ThF}_4\text{-}^{233}\text{UF}_4$, the initial fraction of ^{233}U being adjusted to have an exactly critical reactor.

TRU-started MSFR

The initial fuel salt is composed of $\text{LiF-ThF}_4\text{-(TRU)F}_3$. More precisely, the reference MSFR is started with a TRU mix corresponding to the transuranic elements contained in an UOX (60 GWd/ton) fuel after one use in a standard LWR and five years of storage. The amounts of TRU elements initially loaded in the TRU-started MSFR are given in Table 3 and their isotopic fraction is detailed in Table 4.

Table 4: Proportions of transuranic nuclei in UOX fuel after one use in PWR without multi-recycling (burnup of 60 GWd/ton) and after five years of storage

Isotope	Proportion in the mix
Np 237	6.3 mole%
Pu 238	2.7 mole%
Pu 239	45.9 mole%
Pu 240	21.5 mole%
Pu 241	10.7 mole%
Pu 242	6.7 mole%
Am 241	3.4 mole%
Am 243	1.9 mole%
Cm 244	0.8 mole%
Cm 245	0.1 mole%

A.II- OPTIMISATION OF CORE GEOMETRY

A.II.1- Neutronic benchmark

A benchmark was performed in the frame of EVOL project to compare the several codes. In this way, a large diversity of important neutronic parameters calculations performed by benchmark participants were compared, while using different tools, databases and methods. An overall good agreement could be observed for the static neutronic parameters as thermal feedback coefficients, delayed neutron fractions, generation times, neutron flux and initial critical composition calculations. Only small discrepancies were thereby observed for the evaluations based on different calculations tools, while the choice of the nuclear database has a more consequent impact on the results.

As mentioned above, during the initial reactor design studies, in particular those related to the neutronic calculations, the MSFR core was approximated as a single compact cylinder (2.25 m high x 2.25 m diameter). The next step is the thermal-hydraulics simulations benchmark. Preliminary thermal-hydraulics calculations performed in the frame of the EVOL project have shown that the simple design used for the first benchmark of neutronic calculations will induce very hot spot in the salt flow. Because it's not efficient to compare results too far from the working point of the MSFR, a more complex geometry has been designed for the thermal-hydraulics benchmark in order to obtain acceptable thermal-hydraulic performances. The main results are presented in the next section.

A.II.2- Alternative MSFR spherical core shape design

The favorable features of the MSFR concept allow a great flexibility in the design of the reactor core. The choice of a particular core shape and of a specific arrangement of the fuel circuit components (pumps, heat exchangers, etc.) can be seen as a compromise between several desirable characteristics. A different core shape (Figure 4) has been studied by INOPRO and POLIMI as an alternative design option for the MSFR, referring to both the full scale reactor and a small demonstrator.

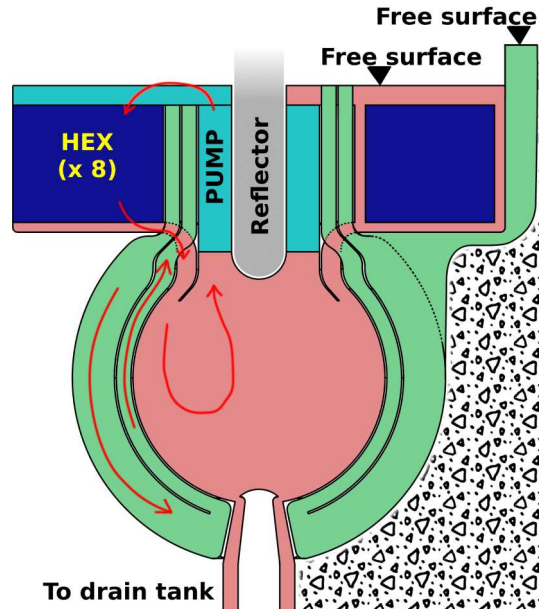


Figure 4: Arrangement of the main reactor components (not to scale)

The present design option has been achieved adopting a “combined” optimization approach, which considers the strongly-coupled behavior of the reactor neutronics and thermal fluid dynamics, according to the following main optimization criteria:

- Ensure good neutron economy and breeding performance
- Avoid hot spots at walls and reduce the overall temperature of structural materials
- Improve the effectiveness of natural circulation under pump blockage accidents
- Keep the design as simple as possible
- Enable easy replacement of the main components of the fuel loop.

The preliminary results of the design optimization process are shown in Figure 4 (not to scale). The cold fuel salt (depicted in pink) is injected at the top of the spherical core. The cold flow goes down staying close to the wall, keeping it at a low temperature, and then rises again and is extracted from the top after being heated from the fission reactions. The salt flows in a vertical riser and enters in the modular pump-HEX blocks.

Coupled neutronics-CFD simulations show that recirculation vortices appear inside the core but are likely to be located far from structural materials. Figure 5 shows the results of a simplified coupled neutronics-CFD simulation of the fuel circuit for the nominal conditions, with reference to the full scale reactor. The simulation has been performed adopting a purpose-made modeling tool based on the open-source C++ finite-volume library OpenFOAM^{12 13}. On the left, the fuel temperature field is

¹² M. Aufiero, A. Cammi, O. Geoffroy, M. Losa, L. Luzzi, M.E. Ricotti, H. Rouch, “Development of an OpenFOAM model for the Molten Salt Fast Reactor transient analysis”, submitted to Chemical Engineering Science (2014)

¹³ O. Geoffroy and M. Aufiero, “A few comments on the MSFR safety and design optimization”, presented at the EVOL WP2 Workshop + EVOL Meeting, Grenoble, France, Available at: <http://indico.in2p3.fr/conferenceOtherViews.py?confId=8432> (2013)

shown along with the flow stream lines. On the right, the neutron flux is depicted. For better clarity, the position of the pump-HEX blocks is also shown.

Previous studies highlighted the necessity to actively circulate and cool the blanket salt. In the present design option, the blanket salt flows in a circuit external to the salt container. This arrangement ensures a very good neutron economy because most of the neutrons escaping from the reactor core are captured in the surrounding blanket. Moreover, the blanket salt (depicted in green in Figure 4) follows a path which improves the cooling of the main metallic structures of the fuel circuit.

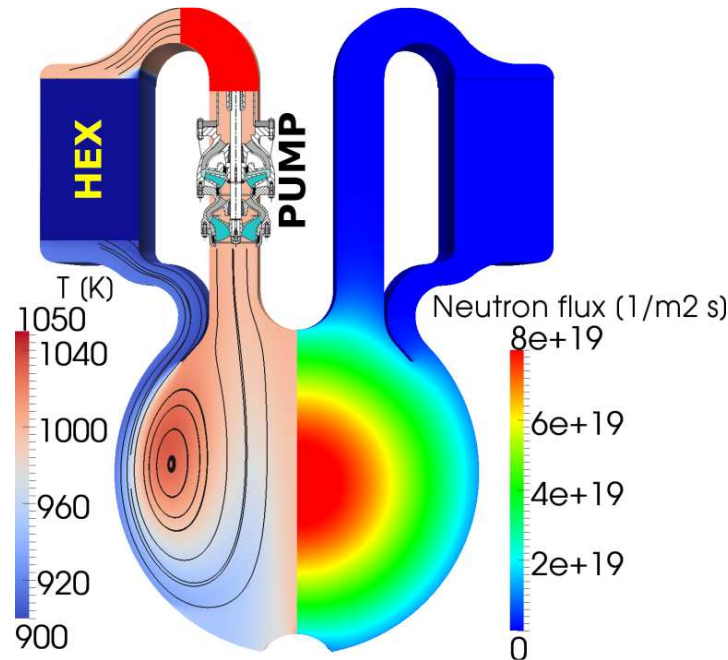


Figure 5: Simplified coupled neutronics-CFD simulation of the alternative spherical core design (nominal conditions, full scale reactor)

The elevation of both the fuel and blanket heat exchangers (the latter being not shown in Figure 5 for simplicity) promotes the establishment of natural circulation in both loops and improves the reactor cooling in case of specific accidental scenarios.

The arrangement of the primary circuit facilitates the removal of the main components for maintenance. Each single modular pump-HEX block could be designed in a way that it can be immersed in the circuit and removed without moving other fuel circuit components, and without completely removing the fuel salt from the core. This is ensured by the accessibility of the blocks from the top free surface of the salt. The secondary salt pipes and the pump motor and shaft are expected to be located above the reactor. The present arrangement would possibly allow a simpler replacement of the fuel salt container (without necessity of direct access to the reactor cavity), which is expected to be required at regular intervals, due to radiation damages.

A.III- RECOMMENDATIONS FOR AN MSFR DEMONSTRATOR PRE-CONCEPTUAL DESIGN

Because the MSFR is a new concept and because of a worldwide lack of expertise in many of the fields concerned, it is impossible to move quickly to a demonstration phase involving actinides acceptable by safety authorities. Prior to that, a variety of experimental setups have to be devised to validate insofar as possible the technological solutions, with non-radioactive or weakly radioactive materials, and demonstrate their viability..

Table 5: Several levels of facilities, in term of size and radioprotection

Sizing of the facilities	3 levels of radioprotection
Small size: 1 liter Chemistry and corrosion studies off-line reprocessing Acquirement of basic data, pyrochemistry CNRS and ITU have already these facilities	Inactive simulant
Medium size: 100 liters Hydrodynamics, noble metal extraction, heat-exchangers, fluorination	Low activity (^{232}Th and depleted U) CNRS and ITU have already these facilities
Full size experiment: 1 m^3 salt/loop Validation of technology integration and hydrodynamic models	High activity ^{233}U , U enriched, MA, Pu Nuclear facilities

In the frame of this R&D, the experimental setups can and should, in the initial phases of the demonstration, be limited in size and complexity (see Table 5) so as to facilitate the necessary modifications that will be associated to the developments. The work with "simulant salt" has to be done for thermal-hydraulic measurements and component tests.

The chemical data determination cannot be done, obviously with simulant. Some facilities available at CNRS and ITU are used at a lab-scale to do measurements with active materials.

A.III.1- Power demonstrator

MSFR demonstrator: preliminary design studies

A 100MW_{th} (or so) demonstrator seems necessary to produce a sufficient amount of gaseous and metallic fission products to test the on-line gaseous fuel processing system. The characteristics of this MSFR demonstrator are listed in Table 6.

The salt volume involved (1.8 m^3) would be one tenth that of the reference reactor (18 m^3) with 60% of the salt in the core, to have a system representative of the reference MSFR in terms of heat exchangers (fluid velocity, thickness of the plates and gap between the plates - both on the side of the fuel salt and of the intermediate fluid), irradiation damages and neutronic behavior. It would be operated during only a few years. The batch reprocessing will thus not be mandatory but the system could provide salt samples useful to test the off-line salt reprocessing (soluble fission product extraction).

Since this demonstrator will be operated during a short time period only, having a self-breeder system is not mandatory. Consequently, and to simplify the design, the fertile blanket will be replaced by a radial inert reflector identical to the axial reflectors. The return circulation of the salt is here divided into 6 loops located around the core, similar to the external loops of the reference MSFR (Figure 6). The design of these 6 loops, especially in the bottom and top regions of the core, may not be same as that of the full scale equipment optimized during the EVOL project. But the design work will be done using the benchmarked procedure for CFD and coupled simulations.

Table 6: Characteristics of the MSFR power demonstrator

Thermal power (MW _{th})	100
Mean fuel salt temperature (°C)	725
Fuel salt heating in the core (°C)	30
Molten fuel salt initial composition (mol%)	LiF-ThF ₄ - ²³³ UF ₄ or LiF-ThF ₄ -(^{enriched} U+MOx-Th)F ₃ with 77.5 % LiF
Fuel salt melting point (°C)	565
Fuel salt density (g/cm ³)	4.1
Core dimensions (m)	Radius: 0.556 Height: 1.112
Fuel Salt Volume (m ³)	1.8 1.08 in the core 0.72 in the external circuits
Total fuel salt cycle in the fuel circuit (s)	3.5

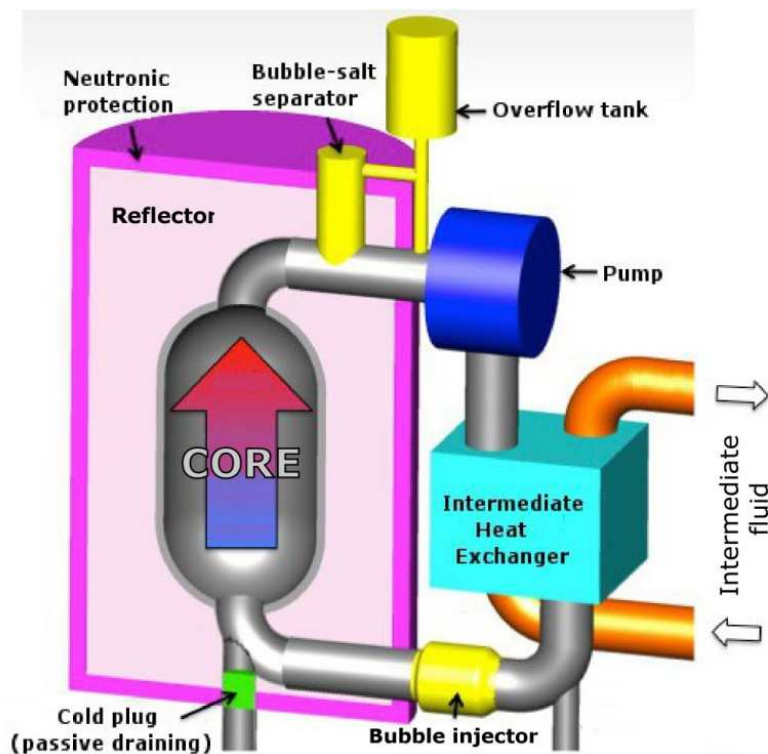


Figure 6: Schematic view of the MSFR demonstrator with one of the 6 external loops

Ideally, if a ²³³U initial load of about 650kg could be made available this would be the simplest way to start such a demonstrator. The evolution of the heavy nuclei inventory in such a ²³³U-started MSFR demonstrator is displayed in Figure 7. The initial fissile is equal to 3.405 mol% in this case.

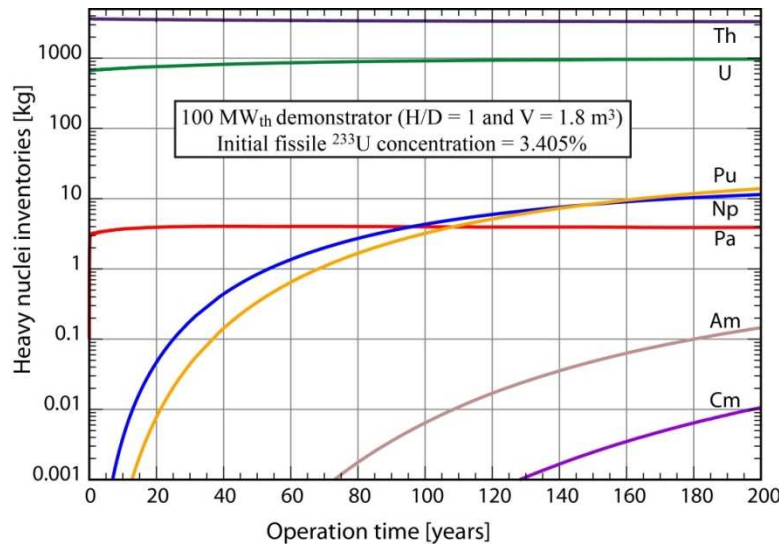


Figure 7: Time evolution up to equilibrium of the heavy nuclei inventory for the ^{233}U -started MSFR demonstrator

A.III.2- From a demonstrator to a modular reactor

At the present time, it seems possible to slightly modify such a demonstrator which could then be a self-breeder modular reactor thanks to the addition of fertile blankets and a slow chemical reprocessing of the fuel salt (1/10th of the reprocessing rate of the reference MSFR). It should be combined with a system to extract the uranium from the fertile blankets in order to provide the fissile matter feed-in. It is interesting to note that such a reactor could be operated at a power of up to 300MW_{th} . This would then be a "modular" reactor that could be exploited commercially. Four parameters have been considered for the evaluation of the breeding capacities of such a reactor, as detailed in Table 7: the power generated (100 and 200MW_{th}), the height/radius (H/R) ratio of the core, the addition (columns labeled 'Radial blanket') or not (columns labeled 'No radial blanket') of a radial fertile blanket around the core, and the impact of the reprocessing rate of the fuel salt between 1 and 4 liters per day. The results written in bold italic in Table 7, where the breeding ratio is larger than or equal to zero, represent the configurations suitable for a breeder reactor. It is to be noted that the trends deduced from the calculations are correct but that the numerical results reported here are impacted by uncertainties on the nuclear data (mainly on the capture over fission ratio of ^{233}U) leading to ± 2 to 3% margins on the breeding ratios.

With a reprocessing rate of 1 liter of fuel salt per day, only the configuration producing 100MW_{th} with a ratio H/R equal to three and including a radial fertile blanket corresponds to an iso-breeder reactor. With a reprocessing rate of 4 liters of fuel salt per day, the two configurations with an elongated core (H/R=3) are breeder.

The addition of an axial fertile blanket above the core on top of the radial fertile blanket has been checked to improve the breeding capacities of the modular reactor. As presented in Table 7, this solution leads to breeder configurations even for a core whose height/radius ratio is equal to 2 (height=diameter). A molten salt modular reactor could be operated at a power of 300MW_{th} in a breeder mode only with such an axial blanket.

Table 7: Breeding capacities of different configurations of a modular MSFR operated during 30 years

	No radial blanket and H/R=2	Radial blanket and H/R=2	Radial blanket and H/R=3	No radial blanket and H/R=2	Radial blanket and H/R=2	Radial blanket and H/R=3
Power [MW _{th}]	100	200	100	200	100	200
Initial ²³³ U load [kg]	654	654	667	667	677	677
Fuel reprocessing of 1l/day						
Feeding in ²³³ U [kg/an]	11.38	23.38	1.72	4.70	-0.07	0.98
Breeding ratio	-29.83%	-30.64%	-4.52%	-6.16%	0.18%	-1.29%
Total ²³³ U needed [kg]	1013.87	1388.37	738.83	835.16	715.05	754.25
Breeding ratio with an additional axial fertile blanket			1.81%	-0.04%		
Fuel reprocessing of 4l/day						
Feeding in ²³³ U [kg/an]	11.20	22.58	1.48	3.58	-0.38	-0.26
Breeding ratio	-29.37%	-29.59%	-3.88%	-4.69%	1.00%	0.34%
Total ²³³ U needed [kg]	1001.86	1353.13	722.50	794.21	709.74	723.03
Breeding ratio with an additional axial fertile blanket			2.49%	1.54%		

A.IV- MOLTEN SALT REACTOR SAFETY ANALYSIS

Three fundamental functions of nuclear safety must thus be ensured in all circumstances:

- control of the chain reaction, thus of the power generated by the fissions;
- evacuation of the energy released by the fuel elements both during reactor operation and after the chain reaction has been stopped (residual heat);
- confinement of all radioactive materials.

Both the probabilistic and the deterministic approach aim at maintaining the risks related to nuclear facilities at acceptable levels.

Two methods: the probabilistic approach and the deterministic approach and Defense in Depth.

The global safety objectives are fully transposable to the MSFR reactor. The difficulty lies in the identification of severe accidents for this type of reactor. The Risk and Safety Working Group (RSWG) is working on the development and demonstration of an integrated methodology that could serve to evaluate and document the safety of generation IV nuclear systems. They have produced a methodology called ISAM which consists in 5 distinct analysis tools intended for use at different stages of the development

Qualitative Safety Features Review (QSR)

Phenomena Identification and Ranking Table (PIRT)

Objective Provision Tree (OPT)

The studies performed in the frame of the EVOL project leads to define a safety approach dedicated to molten salt reactor, that means considering that the fuel is liquid and flows in the reactor. A "cold plug" at the bottom of the reactor vessel has been designed for passive safety issue. This leads to drainage of the core when it fuses (in case of electrical shut down or strong temperature increase). The three confinement barriers were defined in the specific frame of the PWR reactor development or, more generally, in the frame of solid-fueled reactors. As a first step and as a pedagogical illustration describing the overall facility, the 3 fuel salt confinement barriers in the MSFR can be identified by analogy with PWRs.

The first fuel salt barrier is called the "fuel casing" (in pink on the figure): the fuel circuit (heat exchangers, pumps) and the draining system (the tank and pipes).

The second barrier: the reactor vessel (light blue): the intermediate circuit and the draining tank.

The third barrier: the reactor containment structure (the building, in grey) and the emergency cooling chimney, not shown on the drawing

A transient analysis was realized and the main conclusions are:

- 3D ULOF calculation results show that with the actual design, the risk of salt solidification in the intermediate heat exchanger appears. This may happen very fast, but mainly due to the non-optimized heat exchanger design. With optimized heat-exchangers and/or other improvements in the MSFR design one may try to prevent a rapid salt solidification. This is a possible subject for future investigations.
- It must be stated here that the performed analyses, do not go deeply into the domain of severe accident scenarios. They do, however, determine which initiators and further additional failures could/maybe lead to severe accident conditions and whether there is a time available to perform corrective actions by e.g. an operator, i.e. whether an accident prevention and management strategy is feasible.
- The results of the different transient analyses demonstrate that the MSFR plant as proposed by EVOL project is a robust reactor with inherent safety features and a high safety potential. Further development of calculation models, accumulation of safety-relevant experimental results, design optimizations and additional safety analyses, in particular for hypothetical severe accidents, would provide a deeper understanding of MSFR safety issues.

A.V- CONCLUSIONS AND PERSPECTIVES

This study introduces the need for several demonstration tools before reaching the final levels of a zero power demonstrator and subsequently a power demonstrator from which an industrial prototype may be defined. Safety consideration by safety authorities should be addressed all along the demonstration process, and this should take time, more than that needed previously for older concepts. This is essential for an innovative reactor concept that has a potentially high level of intrinsic safety.

Two designs have been presented for the final step of the power demonstrator. For the MSFR-like demonstrator, a rather small reactor would both fit the needs for a demonstrator and be the base for modular reactors (300MW_{th}) with less than 2 cubic meters of fuel salt. A simplified version of such a small reactor would be a burner only reaching fissile regeneration with an additional fertile blanket. It may be the simplest prototype to build and operate. An alternative spherical core shape design has been also introduced, taking into account the strongly-coupled behavior of the reactor neutronics and thermal fluid dynamics. It is characterized by an arrangement of the fuel circuit that would still ensure good neutron economy and breeding performance, limit hot spots at walls and reduce the

overall temperature of structural materials, improve the effectiveness of natural circulation under pump blockage accidents, and keep the design as simple as possible. Preliminary analyses of the pre-conceptual spherical core shape design have demonstrated such potentialities, it could be further investigated.

At this point, several design and fuel composition options are still open after the EVOL-MARS collaboration. This is an illustration of the high flexibility of this concept both in terms of size and fuel composition. Proceeding further in the definition of the most suitable common demonstrator for all the foreseeable application of this concept, with priority to simplicity and compliance to the safety authority requirements will be an important next step of future international collaborations.

B.I- FUEL CHEMISTRY

B.I.1- Selection of a fuel salt composition

The selection of a fuel salt composition was a milestone of the project and a key point for the deployment of MSFR concept. The right choice of the fuel salt is very complex issue as many criteria must be taken into account. This includes the neutronic properties, thermo-chemical properties with major emphasis on the melting temperature, clean-up issues, as well as corrosion and redox control mechanisms.

The fuel for MSFR is a multi-component fluoride mixture which has been proposed based on past experience from the ORNL, novel neutronic calculations and general physico-chemical properties of the fluoride salts. Components that must be considered for the start-up salt are ThF_4 , UF_4 and PuF_3 , in which ThF_4 is represented by ^{232}Th isotope and serves as fertile material to breed ^{233}U , UF_4 is fissile material, but its presence is important for the control of the redox potential of the fuel via the UF_4/UF_3 ratio, and PuF_3 is the primary fissile material, mainly represented by the ^{239}Pu isotope. These three 'must be presented' components are dissolved in a molten fluoride matrix and the choice and exact concentration of all the components are selected based on the following criteria:

- Neutronic properties; the fuel must allow the reactor to be critical, insure intrinsic stability of the reactor through good safety parameters (thermal feedback coefficients and a large enough fraction of delayed neutrons), and possibly give positive breeding gain.
- Melting temperature; general rule is that the lower the melting temperature, the better it is as it reduces the chance of a system freezing. Lower melting temperature also allows lower operating temperature of the reactor and that is important, as it decreases the corrosion rate of the structural material by the fluoride salt (e.g. chromium leaching from Ni-based alloys)
- Redox potential; the fuel salt must be maintained within a certain redox potential so it inhibits the corrosion of the structural materials.
- Reprocessing scheme; Various components of the fuel salt must fit the reprocessing scheme to keep the fuel clean-up process efficient and reasonably possible.
- Physico-chemical properties like viscosity, thermal conductivity or density must be taken into account to keep efficient fuel flow and the heat transfer.
- Economics; the components of the fuel matrix must be cost efficient to make the reactor economically interesting.

The initial fuel composition of the Pu-started MSFR was based on dissolution of 5 mol% of PuF_3 in ^{7}LiF - ThF_4 eutectic (78-22 mol% composition). The melting temperature of such fuel is 935 K (662 °C) which is believed to be too high, moreover such fuel would not contain UF_4 which is needed to control the redox potential of the salt via setting the UF_4/UF_3 ratio, as discussed above. For these two main reasons one of the tasks (and milestones) of the EVOL project was to optimize the fuel for MSFR which has been done in several stages as described below.

Stage 1

To lower the melting temperature of the MSFR fuel at the first stage we have looked for an alternative matrix component to be added to LiF. From the past experience, mainly performed at ORNL in the 1960's, somewhat limited choice of compounds has been considered: NaF, KF, RbF, BeF₂ and CaF₂. The argumentation why these compounds have been primarily considered as potential candidates and the reasoning whether they can be part of the fuel is given below, treating each of the compounds individually.

- NaF, KF, RbF: poorer neutronic properties and problematic for reprocessing. Therefore, these three candidates have been disregarded.

- BeF₂: BeF₂ has a very low neutron capture cross section and the eutectic between LiF and BeF₂ is very low, at 636 K (363 °C). All these three aspects are favourable for the MSFR fuel, but the fact that there is very low solubility of ThF₄ and PuF₃ in BeF₂-containing salts makes it not feasible for such application, since the required amounts of fertile ThF₄ and fissile PuF₃ are rather high, around 20 mol% and 5 mol% respectively. As an example, addition of 20 mol% ThF₄ into the LiF-BeF₂ eutectic increases the melting temperature from 363 °C to 740 °C. It is thus concluded that BeF₂ is not a suitable candidate to lower the melting temperature of the MSFR fuel due to rather high concentration of actinide fluorides.

CaF₂: CaF₂ is suitable candidate from the reprocessing point of view, but is not as favourable from the neutronic aspects. Moreover, addition of CaF₂ will not lower melting temperature of the MSFR fuel.

Stage 2

As it was not possible to find an additional matrix component of the MSFR fuel we have sought the opportunity to optimize the fuel choice with respect to melting temperature using the thermodynamic database describing the LiF-ThF₄-UF₄-PuF₃ system.

Taking the advantage of the complete thermodynamic database we have calculated the lowest melting temperature in the LiF-ThF₄-PuF₃ system. This is highlighted in Figure 8 showing the liquidus projection of the LiF-ThF₄-PuF₃ system indicating the lowest eutectic at 817 K and the LiF-ThF₄-PuF₃ (74.9-22.3-2.8) composition. Such temperature is very low, but does not contain enough PuF₃ to have a critical reactor. We therefore had to increase the content of fissile material which consequently increases the melting temperature of the fuel as described further.

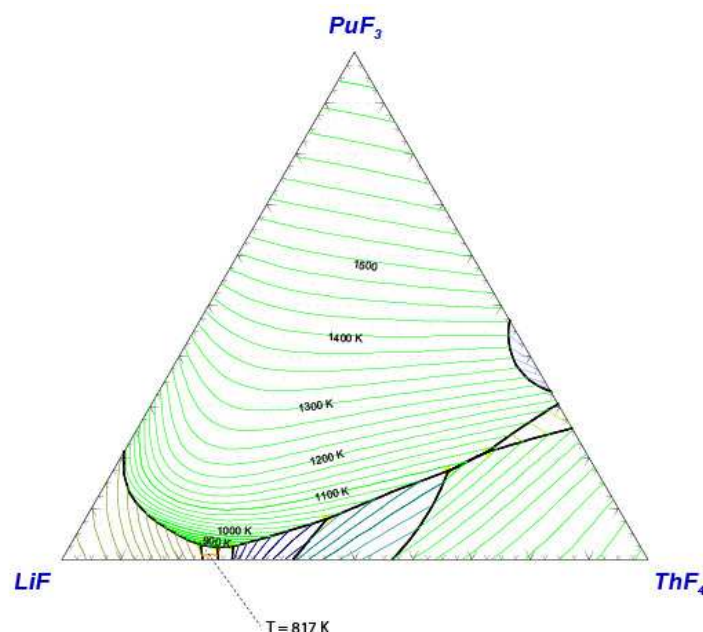


Figure 8: A calculated liquidus projection of the LiF-ThF₄-PuF₃ system indicating the lowest melting temperature at 817 K and LiF-ThF₄-PuF₃ (74.9-22.3-2.8) composition.

Option 1

As stated above the initial fuel composition of the MSFR is based on the LiF-ThF₄ (78-22 mol%) solvent with addition of 5 mol% PuF₃ with melting point 935 K. We must note here that presence of UF₄ and UF₃ components is mandatory in order to control the redox potential of the fuel salt via the right ratio of the two components. However, since UF₄ has very similar melting behaviour as ThF₄ and because its concentration does not have to be necessary high (~1 mol%) the melting temperature will be negligibly affected by this addition. Furthermore, the concentration of UF₃ is around 100 times less than that of UF₄ and thus will have no influence on melting behaviour as well.

From the above given perspectives, the LiF-ThF₄-UF₄-PuF₃ (78.6-15.4-1-5 mol%) composition could be suggested as promising candidate for the MSFR start-up salt, but according to neutronics this would require enrichment of ²³⁵UF₄ largely too high due to non-proliferation issues. In the next step, it has been checked from a neutronic point of view that the Uranium enrichment necessary to have a critical reactor, does not have to be initially too high regarding non-proliferation issues.

As conclusion of this study, to decrease the level of enrichment to acceptable 20% the total concentration of UF₄ had to increase to 3.5mol%. It has been confirmed by neutronics that the proportional amount can replace ThF₄ to become **LiF-ThF₄-UF₄-PuF₃ (78.6-12.9-3.5-5 mol%)** composition. With melting temperature of 873 K and considering a safety margin of at least 50 K the inlet temperature of the reactor would be 923 K. The output temperature is to be defined according to the reactor design, but with reasonable increase of another 50 K would be 973 K which would be considered as maximum reached temperature in the primary circuit under normal operating conditions. This value is compared with the temperature that is required in the reprocessing chemical plant and which is determined by the salt composition during the clean-up process. In fact, it may be necessary to remove the fissile material prior to fission products and that would result into a salt composition of LiF-ThF₄ (85.9-14.1) with melting temperature of 998 K. This value must be treated with care as with the same applied safety margin avoiding the system freezing would it results into temperature around 1050 K.

Such high temperature is of concern, but it must be noted that the demand on low temperature is much higher in case of the reactor compared to the reprocessing vessel, as other structural materials (e.g. graphite or ceramics for coatings ...) or e.g. cold crucible technologies may be used during reprocessing. Furthermore, the exact reprocessing scheme is not yet exactly defined and it may be that the clean-up process will not require such dramatic composition shift of the fuel.

Option 2

The second fuel option proposed in this deliverable is based on lower initial concentration of PuF₃ which would be compensated with corresponding amount of fissile UF₄ sufficient to have a critical reactor and to keep the breeding ratio above 1. The lower actual concentration of PuF₃ in the reactor would result in lower melting temperature. Coupling the neutronic and thermodynamic calculations the **LiF-ThF₄-UF₄-(TRU)F₃ (77.5-6.6-12.3-3.6)** composition, in which TRU stays for transuranium elements (3.15mol% - PuF₃, 0.23mol% - NpF₄, 0.19mol% - AmF₃ and 0.03mol% - CmF₃) has been identified as suitable fuel composition from both points of view. The calculated uranium enrichment is 13% ²³⁵UF₄ and is generally acceptable from the non-proliferation point of view. The above given composition is considered as another option for the start-up fuel for the MSFR with melting temperature of 857 K which is somewhat lower compared to the 'Option 1' discussed above.

Regarding safety issues, the Uranium enrichment of the initial fuel salt has only a slight impact on the safety coefficients which remain comfortably negative for all the MSFR configurations started with enriched U and TRU

However, on the other hand the melting temperature of the corresponding LiF-ThF₄ solvent free of actinides (LiF-ThF₄ (92.2-7.8)) which may be present in the reprocessing plant after actinide separation would be higher, corresponding to 1072 K.

CONCLUSION

Based on the investigation of the optimal fuel selection for the MSFR concept coupling the thermodynamic approach and the neutronic calculations two fuel options have been identified. Their compositions are given below highlighting their advantages and drawbacks:

Option 1 - LiF-ThF₄-UF₄-PuF₃ (78.6-12.9-3.5-5 mol%)

Advantages: low melting temperature in the reactor, breeding ratio above 1

Drawbacks: increased temperature needed in reprocessing plant

Option 2 - LiF-ThF₄-UF₄-(TRU)F₃ (77.5-6.6-12.3-3.6)

Advantages: low melting temperature in the reactor, breeding ratio above 1

Drawbacks: relatively high temperature for reprocessing.

B.1.2- Physico-chemical properties of the fuel salt

To design a nuclear reactor the knowledge of physico-chemical properties of the fuel is required. In this deliverable we will report thermo-chemical properties of the two optimized fuel composition for the MSFR which were proposed in Deliverable 3.7. The two compositions are:

Fuel 1: LiF-ThF₄-UF₄-PuF₃ (78.6-12.9-3.5-5 mol%)

Fuel 2: LiF-ThF₄-UF₄-(TRU)F₃ (77.5-6.6-12.3-3.6)

and in the case of Fuel 2 TRU represent the transuranium elements which are mainly represented by PuF₃.

The relevant properties of interest which are presented in this study and the motivation of their importance within the MSFR project are listed below:

- melting point: the melting point of molten salt reactor should be as low as possible, as it allows lower operating temperature of the reactor, thus inhibits corrosion and at the same time it lowers the risk of system freezing under certain circumstances.
- vaporization behaviour: the vapour pressure of the MSFR fuel at operating temperatures should be low to avoid evaporation of fuel material. Attention must be made to the composition of the vapour which determines composition shift of the fuel salt via vaporization mechanism. Furthermore, the higher the boiling point the better it is from the safety point of view.
- heat capacity: in general, the higher the heat capacity, the more heat can be stored in the fuel medium and the larger heat margin is achieved during accidental scenario. Higher heat capacity is also fruitful for more efficient heat transfer from the reactor to the heat exchanger.
- thermal conductivity: the higher the thermal conductivity the more homogeneous distribution of the heat will be achieved in the fuel cycle, avoiding big temperature gradients.
- density: important parameter to determine the neutronic behaviour of the fuel
- viscosity: should be as low as possible as it allows smoother flow of the fuel through the reactor circuit

It was not possible to experimentally determine all above given properties for the two selected salts, but with the knowledge of data measured in the past on similar systems coupled with some present simulations we could make reasonable estimates which we describe in the next section individually for each property.

MSFR FUEL PROPERTIES

Melting behaviour:

The melting temperatures of the MSFR fuel compositions were determined using the ITU thermodynamic database which was validated by series of calorimetric measurements performed on selected LiF-ThF₄-CeF₃ samples. Figure 9 shows the determination of the melting temperature of **Fuel 1** composition based on the pseudo-binary LiF-ThF₄ system calculated for fixed amounts of UF₄ and PuF₃ at 3.5 mol% and 5 mol% respectively. As observed, the liquidus temperature (the most upper line in the figure) found at 12.9 mol% of ThF₄ and 78.6 mol% of LiF corresponds to **872 K** which is also the lowest melting temperature on the calculated phase diagram. For clarity the other lines in the

phase diagram represent various sub-liquidus phase equilibria which define crystallization paths upon cooling.

Similar analysis has been done for the **Fuel 2** composition and the calculated pseudo-binary LiF-ThF₄ system with fixed concentrations of UF₄ and PuF₃ at 12.3 mol%, resp. 3.6 mol% is shown in Figure 10. Based on the figure the determined melting temperature of Fuel 2 is **854 K**.

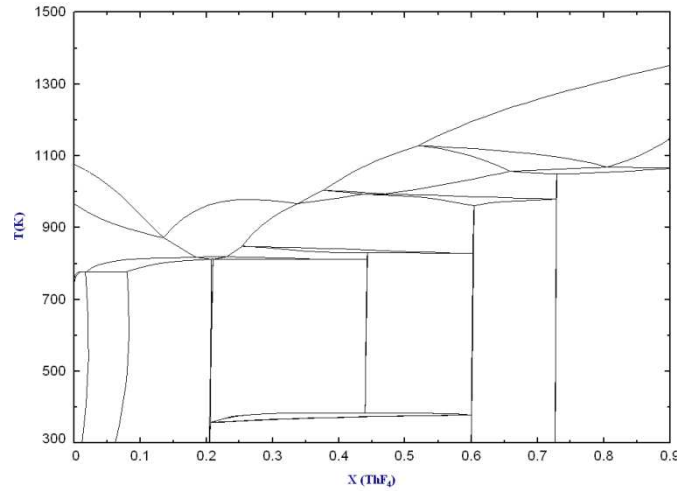


Figure 9: Calculated pseudo-binary LiF-ThF₄ system calculated for fixed amounts of UF₄ and PuF₃ at 3.5 mol% and 5 mol% respectively

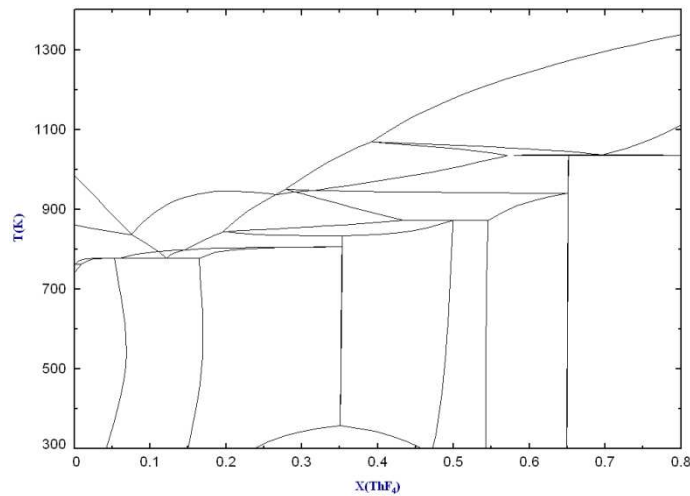


Figure 10: Calculated pseudo-binary LiF-ThF₄ system calculated for fixed amounts of UF₄ at 12.3 mol% and PuF₃ at 3.6 mol%.

Vapour pressure:

Using the thermodynamic database with the assessed data of the liquid phase the vapour pressure was determined from the Gibbs energy difference between the liquid phase and the equilibrium gas phase according to general equation:

$$G(g) - G(liq.) = -RT \ln p(g).$$

The calculated total vapour pressures of Fuel 1 and 2 with corresponding speciation are shown in Figures 11 and 12 respectively. Furthermore, the total vapour pressure was identified for the likely output temperature of the MSFR ($T = 1000$ K) and was found low at 0.07 Pa for both fuel compositions. The calculated boiling points for respective fuel compositions are **2028 K** and **2015 K**.

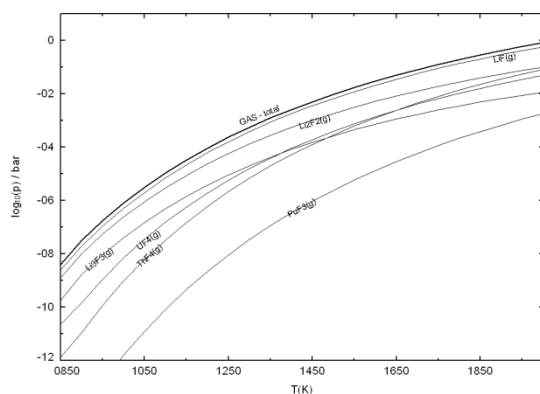


Figure 11: Calculated vapour pressure and its speciation for Fuel 1.

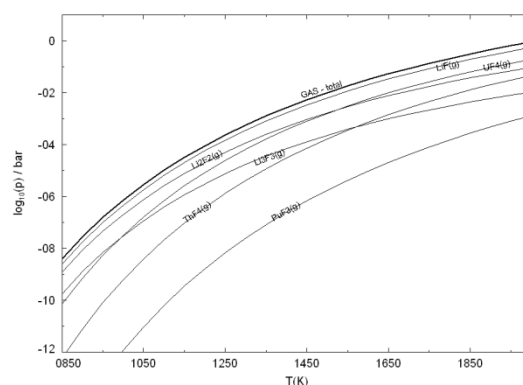


Figure 12: Calculated vapour pressure and its speciation for Fuel 2.

Heat capacity:

The most straight forward way for the estimation of the heat capacity of a multi-component system is by applying the Neumann-Kopp rule which estimates the end value by proportional weights of the end-member contributions. Using such rule the heat capacity of Fuel 1 would be calculated from its end-members as:

$$C_p(1) = 0.786 \cdot C_p(\text{LiF}) + 0.129 \cdot C_p(\text{ThF}_4) + 0.035 \cdot C_p(\text{UF}_4) + 0.05 \cdot C_p(\text{PuF}_3)$$

and the heat capacity of Fuel 2 as:

$$C_p(2) = 0.775 \cdot C_p(\text{LiF}) + 0.066 \cdot C_p(\text{ThF}_4) + 0.123 \cdot C_p(\text{UF}_4) + 0.036 \cdot C_p(\text{PuF}_3).$$

Since the heat capacities of liquid phases of all end-members are constant with respect to temperature the calculated values for the two proposed fuels are constant as well and using the equations above would become $86 \text{ J} \cdot \text{K}^{-1} \cdot \text{mol}^{-1}$ for Fuel 1 and $88.5 \text{ J} \cdot \text{K}^{-1} \cdot \text{mol}^{-1}$ for Fuel 2. However, as it was found in our earlier study¹⁴, there is significant excess contribution in fluoride mixtures which strongly depends on the difference of radius size of lithium cation and other mixing cations. Taking into account this phenomenon we estimate the heat capacity as **$87.8 \text{ J} \cdot \text{K}^{-1} \cdot \text{mol}^{-1}$ ($1.02 \text{ J} \cdot \text{K}^{-1} \cdot \text{g}^{-1}$) for Fuel 1** and **$90.9 \text{ J} \cdot \text{K}^{-1} \cdot \text{mol}^{-1}$ ($1.01 \text{ J} \cdot \text{K}^{-1} \cdot \text{g}^{-1}$) for Fuel 2**. The values for specific heat are also in a very close agreement to the value estimated in our previous study¹⁵ for the LiF-ThF₄ (78-22) eutectic.

Thermal conductivity:

Generally there is lack of data on thermal conductivity for LiF-AnF_x systems and there is no straight forward way to extrapolate this quantity in a multi-component system. In our previous work³⁸ we have related the experimentally determined thermal conductivities of several different fluoride salts to the total content of cations with valence state bigger than 1. Taking into account that Fuel 1 contains 21.4 mol% of AnF_x and Fuel 2 22.5 mol% using such approach the estimated thermal conductivity becomes the same for both fuels, thus **$1.7 \pm 0.4 \text{ W} \cdot \text{m}^{-1} \cdot \text{K}^{-1}$** . The given value is valid for temperature 1000 K and knowing that the used method of extrapolation gives a rough estimate we assign it with increased uncertainty. The estimated value is somewhat higher than the calculated value obtained by molecular dynamics simulation for the LiF-ThF₄ (78-22 mol%) composition which revealed $1.22 \pm 0.81 \text{ W} \cdot \text{m}^{-1} \cdot \text{K}^{-1}$.

Density:

In our previous study³⁸ we have performed analysis of measured densities performed for several different fluoride systems and it has been observed that all densities followed ideal or close to ideal

¹⁴ M. Beilmann, O. Beneš, E. Capelli, V. Reuscher, R. J. M. Konings, Th. Fanghänel, Excess heat capacity in liquid binary alkali-fluoride mixtures, Inorg. Chem. 52 (2013) 2404-2411

¹⁵ O. Beneš, R. J. M. Konings, Thermodynamic properties and phase diagrams of fluoride salts for nuclear applications, Journal of Fluorine Chemistry, 130 (2009) 22-29.

behaviour, i.e. that the density can be extrapolated by averaging the molar volumes of the corresponding end-members. In case of the fuel compositions studied in this report the molar volume is calculated according to:

$$V_M(1) = 0.786 \cdot V_M(\text{LiF}) + 0.129 \cdot V_M(\text{ThF}_4) + 0.035 \cdot V_M(\text{UF}_4) + 0.05 \cdot V_M(\text{PuF}_3)$$

for Fuel 1 composition and according to:

$$V_M(2) = 0.775 \cdot V_M(\text{LiF}) + 0.066 \cdot V_M(\text{ThF}_4) + 0.123 \cdot V_M(\text{UF}_4) + 0.036 \cdot V_M(\text{PuF}_3)$$

for Fuel 2. Knowing molar volume for each of the composition the density (ρ) is calculated from:

$$\rho = V_M \cdot M.$$

Using such approach the density of Fuel 1 becomes:

$$\rho = 5155 - 0.8331 \cdot (T / K) \quad \text{kg} \cdot \text{m}^{-3}, \quad \text{while the density of Fuel 2 is:}$$

$$\rho = 5108 - 0.8234 \cdot (T / K) \quad \text{kg} \cdot \text{m}^{-3}.$$

Viscosity:

The viscosity was determined from the molecular dynamics simulations which were for simplicity performed on proxy system for both fuel compositions. The calculations were done on the LiF-ThF₄-LaF₃ system, in which ThF₄ substitutes UF₄, thus its concentration is equal to the sum of ThF₄ and UF₄ presented in the fuel and LaF₃ represents PuF₃. The principles of molecular dynamics simulation were described in details in Deliverable 3.1 to which we refer for more details. The obtained value for Fuel 1 and Fuel 2 are respectively: $\ln \eta = 0.178 + \frac{403.5}{T-804.2}$ mPa's and $\ln \eta = -0.48 + \frac{771.2}{T-765.2}$ mPa's. Both equations are valid for temperature range 973 - 1273 K. The obtained temperature functions of viscosity are compared with the values extrapolated from the experimental data of Chervinskij et al.¹⁶ who measured viscosity in LiF-ThF₄ and LiF-UF₄ binary salts as function of composition for the whole composition range at 1273 K. The values for the Fuel 1 and Fuel 2 compositions estimated based on this study are 3.4 mPa's and 2.6 mPa's respectively and are correlated with the results of molecular dynamics simulation.

B.1.3- Conclusion

The physico-chemical properties which are recommended for the two MSFR fuel compositions are summarized in Table 8.

Table 8: Physico-chemical properties of the MSFR compositions.

Property	Fuel 1 LiF-ThF ₄ -UF ₄ -PuF ₃ (78.6-12.9-3.5-5)	Fuel 2 LiF-ThF ₄ -UF ₄ -PuF ₃ (77.5-6.6-12.3-3.6)	T range (K) (if applicable)
melting point	872 K	854 K	
boiling point	2028 K	2015 K	
vapour pressure (bar)	$\ln p = 14.263 - 28469/T$	$\ln p = 14.466 - 28701/T$	800 - 2000
heat capacity	1020 J·K ⁻¹ ·kg ⁻¹	1010 J·K ⁻¹ ·kg ⁻¹	800 - 1000
thermal conductivity	$1.7 \pm 0.3 \text{ W} \cdot \text{m}^{-1} \cdot \text{K}^{-1}$	$1.7 \pm 0.3 \text{ W} \cdot \text{m}^{-1} \cdot \text{K}^{-1}$	1000 K
density	5155 - 0.8331 T	5108 - 0.8234 T	800 - 1100 K
viscosity (mPa's)	$\ln \eta = 0.178 + \frac{403.5}{T-804.2}$	$\ln \eta = -0.48 + \frac{771.2}{T-765.2}$	973 - 1273 K

¹⁶ Yu. F. Chervinskij, V. N. Desyatnik, A. I. Nechaev, Zh. Fiz. Chem. 56 (1982) 1946-1949.

B.II- RECOMMENDATIONS OF A REPROCESSING SCHEME

B.II.1- Definition of the reprocessing scheme

One objective of the project was to define, validate and give efficiencies of the steps of the fuel reprocessing in MSFR concept and to indicate the status of the work about the behavior of each element involving in the core (because produced by the fission reaction) at the several steps of the reprocessing.

This work permits also to establish the list of properties required to calculate the efficiency of the extraction steps and a list of missing data (activity coefficient, solubility, redox potential...) will be given.

The reprocessing scheme of the MSFR used fuel is given in Figure 13.

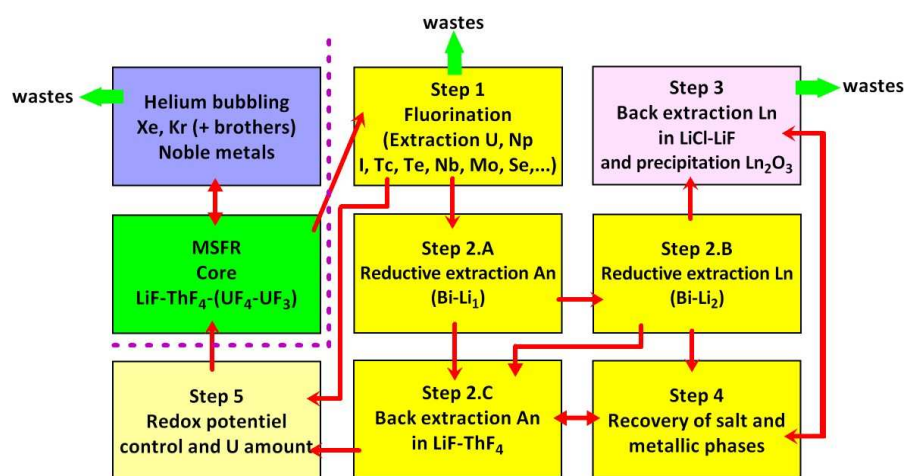


Figure 13: reprocessing scheme of MSFR fuel salt.

The reprocessing is constituted of 2 parts: an on-line reprocessing which consists in bubbling Helium in the fuel salt and an off-line reprocessing which consists in removing *every day about 40 liters* of fuel salt for a special reprocessing in which several steps are involving based on the redox and acido-basic properties of elements in the fuel salt. Because the different elementary steps involving in this process are based on the chemical properties of the elements in the fuel salt, a lot of basic data are required to calculate the efficiency of each step as it will be shown below.

Unlike the concept MSBR developed by the Oak Ridge National Laboratory (ORNL) in the 1960's^{17,18} which operates in a thermal neutron spectrum, the removal of ²³³Pa is not an issue in the MSFR concept because it operates in a fast neutron spectrum. Indeed, due to the neutron captures occurring with ²³³Pa and FPs in a thermal neutron spectrum, the optimized rate of reprocessing was about 4000l/day for the MSBR concept. Therefore, for MSFR concept, the reprocessing rate is strongly decreased due to the fast neutron spectrum, from 4000 l/day in the MSBR concept to 40 l/day in the MSFR. Moreover, no dedicated step for ²³³Pa removal is required in the scheme.

¹⁷ Bettis, E.S., Robertson, R.C., "The design and performance features of a single-fluid molten salt breeder reactor. Nucl. Appl. Technol.", 8 (1970) 190–207

¹⁸ Whatley, M.E., McNeese, L.E., Carter, W.L., Ferris, L.M., Nicholson, E.L. "Engineering development of the MSBF fuel recycle", Nucl. Appl. Technol., 8 (1970) 170–178

B.II.1- Definition of the reprocessing scheme

On-line reprocessing: Helium bubbling

This step has two main advantages: removal of gaseous fission products Xe and Kr and removal of noble metals produced in the reactor core under their metallic states (solid state).

This step has already been studied by the ORNL. In the frame of the EVOL project, the work is especially dedicated to test in a forced convective loop (under construction in CNRS-Grenoble) the efficiency of the bubbling on the solid fission products (noble metals) extraction.

About 15% of the gaseous fission products have a life time very short and will decrease in the salt. The others, about 85% have a life time long enough to be extracted and treated.

The experimental studies of the ORNL have shown that iodines, tritium, krypton and xenon were extracted using this method.

The gas outlet flows through a storage tank during 2 hours. Then the gas flows through an activated carbon trap during 47 hours. In the storage tank, some noble metals are also: Nb, Rh, Mo, Ru, Ta and Te. The radioactive gas ^3H , Kr and Xe flows through this tank and their daughters are trapped in this tank: Ba, La, Cs, Rb, Sr, Y and Zr. Iodines are totally removed in the activated carbon trap.

A scheme of the installation is given Figure 31.

Off-line reprocessing: STEP 1- Fluorination

This step has already been studied by the ORNL and the results obtained can be used for the MSFR reprocessing. The principle of the technique is to oxidize all the elements contained in the salt to their higher oxidation states in order to produce gaseous elements. That is the case of U, Np and some other elements. The gaseous elements are naturally separated from the salt. To avoid the corrosion of the structural material, the wall of the reactor is cooled by a NaK coolant. That leads to the formation inside the reactor of a frozen wall of salt which protects the materials against corrosion.

A part of Pu can also be oxidized in certain condition¹⁹. This step aims at removing the elements with high gaseous oxidation states, such as U, Np, Pu for the actinides and Nb, Ru, Te, I, Mo, Cr, Tc for the fission products. After extraction, the elements are separated in NaF traps heated and cooled at given temperature to perform the separation and extraction processes.

In the last step, actinides which were extracted by fluorination, such as U, Np (and probably a part of Pu), are reduced using hydrogen gas and introduced back in the fuel salt. Only a part of UF_4 is re-introduced, the other part is stored to feed new reactors. All the gaseous elements removed by fluorination are reduced to their solid state using hydrogen gas before storage.

Off-line reprocessing: STEP 2A and 2b- reductive extraction

Because a lot of data obtained by the ORNL can be used for MSFR reprocessing concerning the steps of fluorination and Helium bubbling, in the frame of the first period of the EVOL project, the work on reprocessing was focused on the separation of lanthanides (Lns) and actinides (Ans) because no data were available for the calculation of efficiency for these steps. This separation was expected to be performing by two steps based on reductive extraction (step 2A for actinides and 2B for lanthanides). The objectives are to have an efficient extraction of actinides without lanthanide extraction during the step 2A and to have, next, an efficient extraction of lanthanides.

The best results validated by experimental determinations are obtained using Bi-Li metallic pools. The compositions of the metallic solvent to perform the extractions are:

- Step 2A (actinides extraction without lanthanide extraction): $(\text{Bi-Li})_{\text{An}} = \text{Bi-Li}(0.1\%)$
- Step 2B (lanthanides extraction): $(\text{Bi-Li})_{\text{Ln}} = \text{Bi-Li}(10\%)$

¹⁹ ORNL-4224 report, Nov 1968.

The efficiency relation and the database established lead to calculate the extraction efficiencies for various elements in the systems LiF-ThF₄ / Bi-Li. Using these data, it is possible to optimize the extraction process parameters as a function of the neutronic constraints of the reactor which assess the level of fuel salt cleaning. Indeed, due to the fast neutron spectrum, the formation of lanthanides in the reactor core is not a major problem for the neutronic point of view, but if the concentration becomes too high, lanthanides will precipitate because of their low solubility in the fuel fluoride melt. Then it is necessary to remove them regularly.

As it was demonstrated ²⁰, when the reducing agent is Li, it is possible to perform the two extraction steps (actinides and lanthanides) by changing the concentration of Li in Bi. The extraction efficiency calculations show that it is difficult in only one stage to remove all the actinides or/and all the lanthanides from the fuel salt. To improve the efficiency and to achieve a full extraction will require several extraction stages. The objective is to remove the elements with an efficiency higher than 99.99% and with a high selectivity (in the case of actinides removal).

The total amount of moles of the element M extracted is given by the following relation:

$$n_{\text{ext}} = n_{\text{init}} * [1 - (1 - \mu(M))^{nbs}]$$

in which n_{ext} and n_{init} are respectively the extracted and the initial number of moles of the element M and "nbs" represents the number of extraction stages.

The optimization of the extraction process parameters, nature and concentration of the reducing agent, number of mole in each phase has been achieved. The optimization of the number of stages can be done taking account of the neutronic constraints of the reactor which assess the level of fuel salt cleaning.

Off-line reprocessing STEP 3- back extraction of lanthanides

The lanthanides are extracted from the metallic pool (Bi-Li)₂ by anodic oxidation of the Bi-Li pool in a dedicated salt constituted of LiCl-LiF (70-30 mol%) so-called LiFCl. The second part of the lanthanides management consists in their precipitation under oxide solid form and separation from the salt. The precipitation is performed by bubbling a gas mixture of (H₂O-Ar), the product of the reaction being a mixture of gas (HCl/HF-Ar) which do not modify the composition of the salt.

Balance of the reprocessing - further reprocessing steps

In the ORNL reprocessing scheme, the balance was not equal to zero. The composition of the solvent metallic pools and of the salts (both fuel salt and salt retained for the back extraction of lanthanides) are continuously modified during the reprocessing. Consequently, an increase of the LiF amount in the fuel salt and a decrease of Li amount in one metallic pool were observed. The Table 9 (see page 65) summarizes the composition of the several phases during the steps of the reprocessing.

To prevent the amount variations of Li in the different salts or metallic solvents, one step has been added to complete the general reprocessing scheme. This step uses a buffer solvent liquid metal which device is given Figure 14.

²⁰ ²⁰ S. Delpech, J. of Pure Applied Chemistry, 85 (2013) 71-87

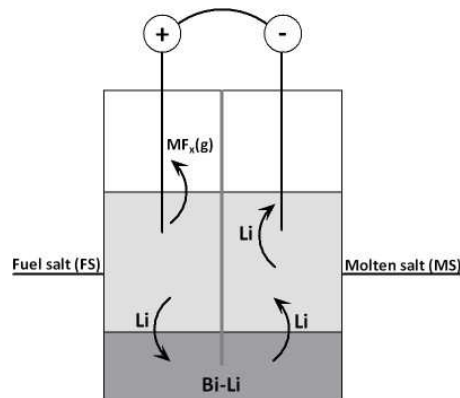


Figure 14: Electrochemical device proposed to remove the excess of LiF due to Ln extraction in the fuel salt

In this way, the LiF concentration of the fuel salt can be modified without modification of another liquid phase.

The device proposed for the back extraction by anodic oxidation of Ans (and Lns) is given figure 15.

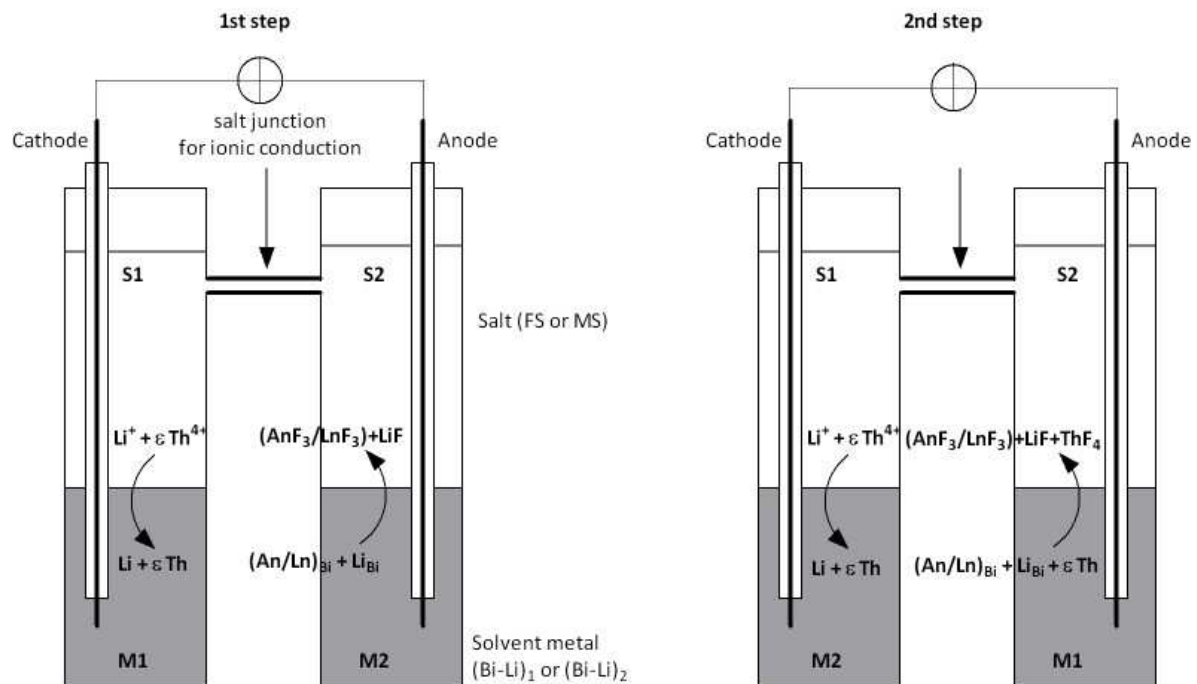


Figure 15: Device proposed for the electrochemical back extraction of Ln and An.

B.II.2- Chemical and physical state of the elements during the reprocessing

The chemical and physical state of the elements depends on the reaction involving in the reprocessing. The elements are fission products. They are produced in the fuel salt, in the reactor core. The fuel salt is maintained at a given redox potential value ranging between -3.3 and -3 V/F₂. That corresponds to a ratio [UF₄]/[UF₃] ranging between 10 and 100²¹. The oxidation state of the fission products (and then its chemical and physical form) depends on their redox properties and on the redox potential of the salt.

After the fluorination steps, all the elements are oxidized to their highest oxidation state which can be reached in the molten salt. In some cases, they can be oxidized to gaseous state.

²¹ S. Delpech, C. Cabot, C. Slim, G. Picard, "Molten fluorides for nuclear applications" (Review), Materials Today, 13 (2010) 36

The reductive extraction and the back extraction steps are based on the redox properties of the elements to be extracted. The chemical reaction of the fission products with the metallic lithium depends on the potential of the redox systems.

The assessment of the behavior of the fission products in the chemical plants requires the knowledge of their chemical properties, redox potentials and solvation properties defined by the activity coefficients of the elements in the fuel salt LiF-ThF₄ and in the solvent metal (Bi).

Combining the thermodynamical data and the activity coefficients, it is possible to calculate the concentration of each element in all the phases. In the frame of the project, we have determined the nature and the state of all the fissions products and their behavior during the reprocessing.

B.II.3- Redox potential control of the salt

Generation IV reactors are currently under investigation and the EVOL program focuses on the Molten Salt Fast Reactor. The fuel is liquid in the concept and considered to be LiF-ThF₄-UF₄.

As the operating temperature should be around 600°C, the chemical resistance of the structural material at high temperature is a crucial point. It was found few decades ago in the MSR program at ORNL that the material corrosion was very sensitive to the redox condition of the fuel salt. That is shown in Figure 16 which presents the corrosion observed at the surface of Ni-based alloys for two different U(IV)/U(III) ratios.

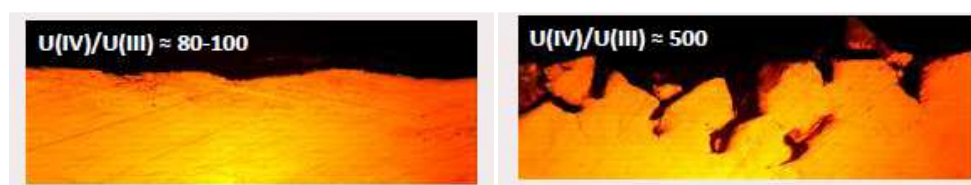


Figure 16: Ni-based alloys after immersion in LiF-ThF₄-UF₄-UF₃ molten salt at 800° for two compositions of U(IV)/U(III)

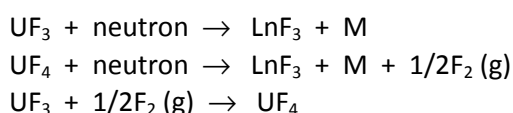
To control the redox conditions, a buffer couple was proposed: U(IV)/U(III). The redox potential of the salt is thus fixed by the uranium species concentrations thanks to the Nernst law:

$$E_{salt} = E_{U(IV)/U(III)}^{\circ} + \frac{RT}{F} \ln \left(\frac{[U(IV)]}{[U(III)]} \right)$$

Where E° is the standard potential of U(IV)/U(III) couple (V), R the ideal gas constant (J/K/mol), F the Faraday constant (C/mol) and [x] the concentration of the x species (mol/L)

To resume, the ratio between U(IV) and U(III) concentrations is thus imposing the salt potential and has to be fixed between 10 and 100.

However, during the reactor operation time, as uranium is the fissile material, its concentration in the salt varies due to the fission reaction²²:

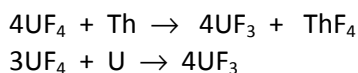


Where LnF₃ is a lanthanide fluoride, M a gaseous product or noble metal, n a neutron

From these equations, the consumption of UF₃ leads to an increase of the [U(IV)]/[U(III)] ratio and thus of the salt redox potential: the consequence is an increase of the chromium corrosion rate.

²² S. Delpech, C. Cabet, C. Slim, G. Picard, "Molten fluorides for nuclear applications" (Review), Materials Today, 13 (2010) 36

A careful control of the redox potential is thus required. A way to limit the corrosion rate, and so to decrease the salt redox potential, is to add a reducing agent in the salt, as U or Th, to consume UF_4 :



In this work, tests on redox potential control were performed in the eutectic LiF-CaF₂ at 850°C using the U(IV)/U(III) redox couple. Metallic uranium was chosen as reducing agent and metal insertion into the salt leads to the following spontaneous reaction:



As expected, the U plate immersion into the molten solution which contains U(IV) ions leads to the formation of U(III). An equilibrium U(IV)/U(III)/U has been reached after 2.5 hours.

To calculate the $[U(IV)]/[U(III)]$ ratio, the U(IV) and U(III) concentrations have to be known. The U(IV) concentration can be evaluated thanks to an electrochemical calibration curve:

$$[U(III)]_t = \frac{4}{3} \{ [U(IV)]_{t=0} \}$$

First of all, the conversion kinetics of U(IV) into U(III) is very fast as the ratio goes from the infinite at the beginning, to 4 within half an hour. The equilibrium obtained after 2.5h in given experimental conditions corresponds to a uranium concentration ratio of 1. As it should be set between 10 and 100 to avoid the core material corrosion, the redox potential of the salt is thus achievable using a U plate as reducing agent.

C.I- STRUCTURAL MATERIALS FOR MSFR CONCEPT

The ORNL laboratory (Oak Ridge National Laboratory) program on the molten salt reactor experiment led to the development of the Hastelloy N alloy, essentially a Nickel ternary alloy with 8wt% of Cr and 12wt% of Mo (Ni-12%Mo-8%Cr-V-Nb)²³. The composition of the alloy was optimized for corrosion resistance (both in a low oxygen gas atmosphere and in molten fluorides), irradiation resistance and high temperature mechanical properties. The material behaves well in fluorides media showing a good corrosion resistance. It also has good mechanical properties up to 750°C but beyond this point, the carbides (VC and NbC) dissolve in the matrix. This promotes grain size coarsening, changes in the mechanical properties as well as a decreased irradiation resistance due to an inefficient helium trapping. While the behavior of this alloy proved satisfactory up to 750°C (a temperature in the low range of the MSFR), it would be impossible to preserve the required material properties in the full operating temperature range required for the MSFR system due to its evolving microstructure at higher temperature. In view of the limitations of the Hastelloy N, the Ni-W-Cr ternary system appears as a promising road to design a high temperature material for molten salt reactors. Replacing molybdenum by tungsten in such alloys is potentially beneficial to reach higher in-service temperature from the point of view of mechanical properties (creep, high temperature strength) while maintaining a suitable corrosion resistance.

Within the framework of the EVOL project, one work package was devoted to the study of a replacement option for Hastelloy N in order to assess the feasibility from the materials points of view of higher in-service temperature. This would be highly desirable to cope with many possible designs

²³ H.E Mc COY et al., Nuclear Appl. & Tech., 8 (1970) 156

of the MSFR. The safety aspects of the MSFR are also an area that would benefit from higher in-service allowed temperatures: being able to with-stand higher temperature in the unwanted case of a power excursion is also beneficial over-all to the safety margins of the MSFR.

The metallurgical key idea is to replace molybdenum with tungsten with the following expected benefits:

- improved creep resistance (the W diffusion coefficient in nickel is roughly 10 times lower than the Mo one ²⁴).
- The replacement of Mo by W does not lead to the formation of detrimental intermetallic phases. A higher concentration of W can be used to further increase mechanical properties.
- Similar or better corrosion resistance in fluorides.
- Lower long-term activation under neutronic irradiation (no 99Tc can be generated).

The activities of EVOL therefore first seek to validate at the industrial scale the processing of suitable NiWCr alloys within a composition range relevant for the MSFR. Second, it is important to establish a database of preliminary results in 2 areas: mechanical properties and corrosion resistance (general corrosion behavior and intergranular Tellurium cracking resistance).

The objective is to evaluate the potential of NiWCr alloys for MSFR. 3 heats (Table 9) have been processed that are being used to perform mechanical tests and corrosion testing. With the ternary composition, it was found that high temperature intergranular cracking occurs which can be mitigated by the addition of deoxidizing elements (Zr for example). The different heats have been characterized at the metallurgical level (microstructure, recrystallization kinetics, sensitivity to IG cracking). One of the heat holds good promise regarding high temperature mechanical properties (EM819).

Table 9: Composition of the three heats performed in the frame of the project

Name	W (wt%)	Cr (wt%)	Mn (wt%)	Al (wt%)	Zr (ppm)	Ti (wt%)	Ni
EM721	25.2	5.7	0.08	0.08	0	0.13	Bal.
EM818	24.6	7.2	Not Evaluated	0.26	0	N.E.	Bal.
EM819	21.7	7.5	N.E.	0.22	350	0.22	Bal.

C.I.1- Metallurgy of NiWCr alloys

The metallurgy of the alloys has been investigated in relatively good details. In particular:

- recrystallization studies have allowed to firmly establish the temperature/duration required during heat treatments.
- the ITE mechanism is apparently not linked to DSA (Dynamic Strain Aging) neither a grain boundary brittle phase nor glide plane decohesion.
- ITE may be related in this alloy to the segregation of an impurity at grain boundaries (before or during testing is not settled). The grain size effect (higher surface to segregate) and the strain rate sensitivity points to such a process. Oxygen is the most likely even so the nanosims study was not conclusive. The fact that EM819 and EM818 contain less dissolved oxygen may explain nicely the better behavior of these alloys compared to EM721.

It has now been clearly established that a ternary composition by itself such as EM721 will not be sufficient to provide a good material. While processing may be achieved, resistance to ITE is jeopardized. It has therefore been shown that microalloying is essential and a candidate material needs to have some deoxidizer such as Zr or Al. It was also concluded that in order to add Zr, some Ti may be necessary at the processing level. The composition of EM819 seems a good compromise

²⁴ T.C. TIEARNAY, N.J. GRANT, Metallurgical Transactions A, 13A (1982) 1827

between strength at high temperature given by the high content of W and resistance to ITE provided the microstructure is further optimized (refined in particular).

Then, the recommended composition for MSFR concept is (in wt%):

W 21.7 - Cr 7.5 - Mn <0.02 - Al 0.22 - Zr 350 (ppm) - Ti 0.22 - Si - Ni Bal
(Mn could be raised if S is an issue)

Forging is going to be a key issue at the industrial scale for 2 purposes:

- high temperature during forging is necessary in order to prevent deep cracking of the heat.
- the amount of deformation to achieve in order to reduce the final grain size is high and is to combine with heat treatment at relatively low temperature. This step still needs to be explored further at the industrial scale in particular the exact sequence should be further investigated.

C.I.2- Mechanical properties of NiWCr alloys

The first significant quantities of NiWCr alloys (EM721, EM818 and EM819 heats) designed for molten salt fast reactor were characterized for mechanical properties. Tensile and creep testing were carried out on the three materials in air. Various tests in compression allowed studying the DSA trend as a function of temperature. The results presented here can be considered preliminary from 2 points of view: the microstructure of these materials is not yet optimized because the definition of the optimum microstructure was available at the end of the EVOL project. A consequence is that the available quantity was limited and only a small number of conditions were worthwhile being studied at this point. However, it is possible to draw preliminary conclusions regarding the mechanical behavior of these materials particularly in comparison with Hastelloy N, its NiMoCr counterpart. It is clear from the tensile tests that the high temperature hardening that was seen in microhardness has been confirmed in tensile and compression testing. It compares well with comparable Hastelloy N material and may be slightly better at the high end of the investigated temperature range. The fracture strain is good at low temperature but changes to very limited strain at intermediate temperature. There is a phenomenon of ITE that wasn't foreseen at the beginning of the program that may require more material development to overcome (the remaining part is to produce an optimized microstructure for EM819 for example). It is clear that microalloying with Zr may present an interesting option to limit the extend of ITE. Indeed, already without optimization, EM819 has a better mechanical behavior than EM721 or EM818 (in its as received state at least). There is a question mark as to whether Al addition is interesting by itself. It was also shown that these alloys (EM721 and EM819) display dynamic strain aging in the intermediate temperature range that may interact with ITE. The creep results are for now rather deceptive as the advantage compared with Hastelloy N is not obvious yet (one negative result and one positive result) but they should be considered as encouraging intermediate results. This calls for more work in this area, particularly when optimized microstructure will be available.

Here we list a set of issues that would be worthwhile investigating further from the mechanical properties point of view.

Short term issues:

- production of optimized microstructure
- investigation of ITE and its mitigation
- creep of optimized microstructure
- investigation of mechanical properties after thermal aging

Long term issue. Since the material is fully optimized yet, we feel that the effect of irradiation on mechanical properties should be a subject for future work but only after this optimization is completed. For example, it is well known that the effect of He is to embrittle grain boundaries in Ni-

W alloys ²⁵. There will be a detrimental effect of He on grain boundaries. The extension of the lifetime of the material will certainly require an optimization of the metallurgy of the NiWCr alloys. It may be controlled through the creation of intragranular trapping interfaces in the material (the effective way is to be defined). The optimization of the microstructure regarding neutron irradiation remains however a major research effort given the relatively limited basis of current knowledge ²⁶.

C.I.3- Corrosion of NiWCr alloys

Experimental corrosion tests evidenced several features related to the corrosion of EM721 (NiWCr) and Hastelloy C260 (NiMoCr) alloys (Table 10) in a LiF-NaF salt polluted by Fe(II) and O(-II):

- Cr selective corrosion occurs in both alloys, as already described in literature ²⁷
- W, and to a lower extent, Mo, are also oxidised
- Fe, most likely reduced from Fe(II) in the salt, diffuses into the alloys
- Hastelloy C260 has a better corrosion resistance than EM721

As Fe(II) was evidenced to play a role in the corrosion mechanism of both alloys, its initial concentration in the salt was varied. An increase of the concentration clearly enhanced corrosion of both alloys, and a suppression of Fe(II) pollution would have been a perfect proof of its role as oxidizing agent. However, Ca metal additions (which clearly reduced the Fe(II) content) lead to an enhanced and so far unexplained corrosion of the alloys.

In pure fluoride systems, the oxidation potential of W/Mo is higher than the oxidation potential of Ni. It is thus suspected that pollution of the salt by O²⁻ also plays a role in the corrosion reaction. Aside from experimental work, thermochemical modeling of the system was thus carried out, in order to evaluate equilibrium composition of the alloys and the molten salt in various conditions, and understand the reason of W and Mo selective oxidation in Ni base alloys.

Table 10: alloys composition

A- EM 721 = wt.% Ni-5.7Cr-25.2W (rods, 5 mm dia.)
B- Hastelloy C276 (wire, 1 mm dia.)
The HastelloyC276 is composed of two phases which were analyzed by SEM-EDX: a matrix (wt.% Ni-7Mo-18Cr-6Fe) and a dispersed phase (wt.% Ni-18Mo-17Cr-7Fe)

Extension of the model to the MSFR salt

Calculations were performed with the MSFR salt (molar composition: 77LiF-16ThF₄-5PuF₃-2UF₄) and the same model alloys Ni-10Mo-10Cr and Ni-10W-10Cr. The purpose was to estimate, depending on the UF₄/UF₃ ratio, which element was expected to oxidize and to dissolve, and to determine the influence of the replacement of W by Mo in structural alloys.

Similarly to previous calculations, a small amount of alloy (2.10⁻³ mol) was equilibrated with a large amount of salt (1 mol), aiming at representing a thin layer of alloy in contact with the salt. However, a major difference with all the work presented in previous sections was introduced: the oxidant was not FeF₂(salt) (which reduces into Fe in the alloy) but rather UF₄(salt) (which reduces into UF₃ (salt)).

The first calculation, presented in Figure 17, was performed with a salt free of oxide. Corrosion products are thus pure fluoride compounds. In this case, Cr is oxidized at UF₄/UF₃ ratio of about 0.2-0.4. Ni starts to oxidize at a ratio of about 1000, while W or Mo do not oxidize for UF₄/UF₃ ratio below 10 000. A small difference in the selective oxidation behaviour of Cr is evidenced between NiWCr and NiMoCr alloys: Cr tends to oxidize a little bit easier in the case of NiWCr alloy. As long as

²⁵ D.K. Matlock and W.D. Nix, Journal of Nuclear Materials 56 (1975) 145

²⁶ A.M. Angeliu, J.T. Ward, J.K. Witter, Journal of Nuclear Materials, 366 (2007) 223

²⁷ J.W. Koger, Effect of FeF₂ addition on mass transfer in a Hastelloy N-LiF-BeF₂-UF₄ thermal convection loop system, Technical report, ORNLTM-4188 (1973)

the UF_4/UF_3 ratio is above 1, it is believed that this difference is of no consequence on the long term behaviour of Ni base alloys, since Cr will diffuse from the bulk of the alloy and eventually end up in the salt.

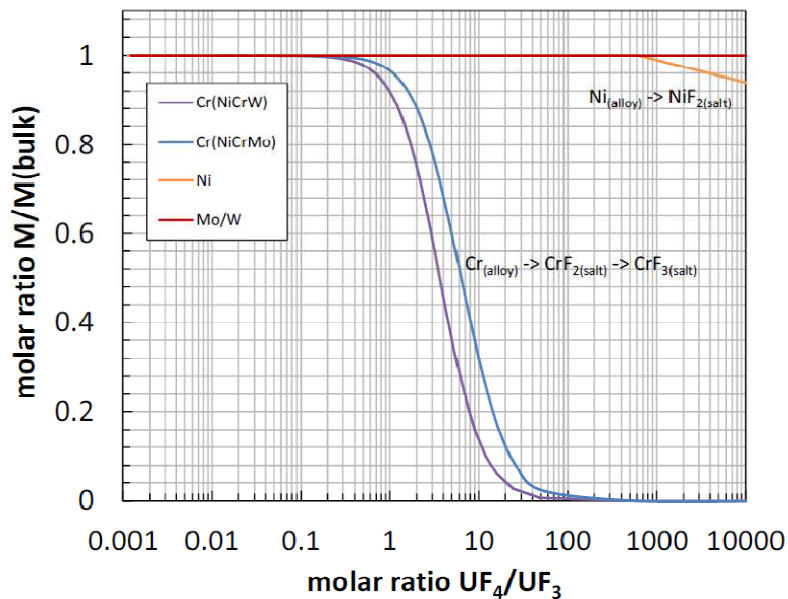


Figure 17: Oxidation behaviour of $Ni_{0.8}W_{0.1}Cr_{0.1}$ and $Ni_{0.8}Mo_{0.1}Cr_{0.1}$ (2 mmol) in $77LiF-16ThF_4-5PuF_3-2(UF_4-UF_3)$ (1 mol) vs. UF_4/UF_3 molar ratio at $750^\circ C$.

This calculation is finally consistent with what is known about Ni base alloys in pure fluoride salts: Cr selectively oxidizes, while Ni, W and Mo are not subject to corrosion at usual UF_4/UF_3 ratio (typically 10-500).

As demonstrated in the LiF-NaF salt, the presence of dissolved oxides is likely to modify the corrosion behaviour of the alloy constituents. A calculation was thus performed by introducing Li_2O in the salt system. The choice of the Li_2O concentration in the salt was driven by the solubility data of UO_2 and ThO_2 , as determined in MSBR salt and summarized by Rosenthal²⁸. Indeed, at $750^\circ C$, and with the MSFR fuel composition ($x(UF_4)=0.02$ and $x(ThF_4)=0.16$), the maximum O^{2-} content is $x(O^{2-})=4.5 \cdot 10^{-4}$ and $x(O^{2-}) = 2.3 \cdot 10^{-3}$ due to UO_2 and ThO_2 precipitation, respectively. The precipitation of UO_2 is thus driving the maximal O^{2-} content in the MSFR salt. The Li_2O concentration was thus fixed at $x=5 \cdot 10^{-4}$ in the calculation.

As evidenced in Figure 18, the presence of Li_2O has a strong influence on the corrosion behaviour of the alloy components:

- Cr oxidation (into $LiCrO_2$) is strongly affected, and occurs even at very low UF_4/UF_3 ratio (~ 0.001)
- Mo and W are oxidized (into MoO_2 and WO_2) at UF_4/UF_3 ratio as low as 0.5
- Ni is also partially oxidized (into NiO).

From the present work based on experimental tests in an inactive LiF-NaF molten salt and on thermochemical modeling of the systems, some important features of corrosion mechanisms of structural NiCrW and NiCrMo alloys can be discussed.

As evidenced in ORNL experiments, the oxidation of structural alloys containing Cr leads to a selective oxidation of this element, which is hardly avoidable in operating conditions, since it would require a too low UF_4/UF_3 ratio.

²⁸ M.W. Rosenthal, P.N. Haubenreich and R.B. Briggs, The development status of molten salt breeder reactors, Technical report, ORNL-4815 (1972).

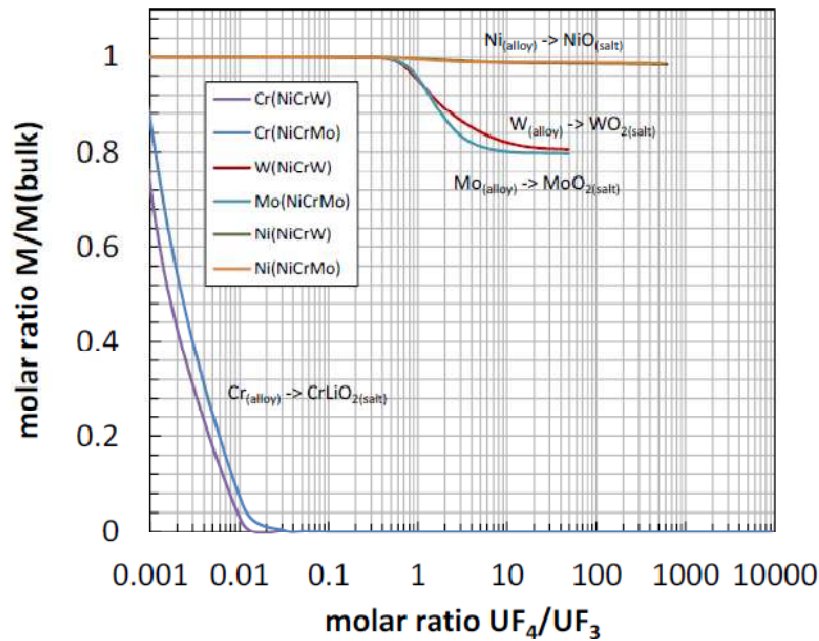


Figure 18 : Oxidation behaviour of Ni0.8W0.1Cr0.1 and Ni0.8Mo0.1Cr0.1 (2 mmol) in 77LiF-16ThF₄-5PuF₃-2(UF₄-UF₃) (1 mol) + Li₂O (5.10⁻⁴ mol) vs. UF₄/UF₃ molar ratio at 750°C.

It was also evidenced in this study that W and Mo suffer from an unexpected selective oxidation. Our conclusion is that this specific corrosion is driven by the combination of two pollutants:

(i) an oxidant, Fe(II), which is reduced into Fe in the alloys, and (ii) dissolved oxides leading to the formation of specific corrosion products (typically Na₂WO₄ and MoO₂). An experimental evidence was clearly established: the increase of Fe(II) concentration lead to an increased corrosion rate. It is believed that the removal of one of this pollutant would strongly decrease (or suppress) corrosion of W and Mo, but, due to the very low concentrations involved (typically about 10⁻² wt.%), this experimental challenge could not be achieved within the project. Finally, both experiments and calculations tend to show that, in LiF-NaF mixtures, NiMoCr alloys have a better corrosion resistance than NiWCr.

However, in the MSFR salt (77LiF-16ThF₄-5PuF₃-2UF₄), calculations show that Mo and W are likely to have a very similar behaviour in the case of oxide pollution in the salt. Indeed, W-containing alloys corrosion seems to be enhanced in the LiF-NaF salt due to the formation of a very stable compound Na₂WO₄ (not formed in MSFR salt since NaF is not a component of the salt).

Nevertheless, in the MSFR salt, thermodynamic calculation indicates that a small oxide pollution (x(Li₂O)=5.10⁻⁴, corresponding to the solubility of UO₂) might also favour the dissolution of W and Mo, even at low UF₄/UF₃ ratio.

C.I.4- Conclusion and recommendations

More work is needed for the processing of NiWCr alloys. A composition is probably defined that takes into account major alloying element (the ternary system NiWCr) and microalloying (additions of Zr notably). Important items have not been investigated that could be part of a future research program:

- processing of large quantities of material at an industrial scale. A further optimization of the material is to be carried out for the realization at the industrial scale of a fine microstructure.
- further enhancement of the composition: the interest of Mn, Nb or rare earth additions could be another direction to look at
- extensive mechanical properties assessment to be done (the work in EVOL was preliminary)
- weldability

- thermal aging at high temperature
- precipitation of W has not been explored thoroughly. It may constitute another metallurgical path to diminish the grain size at the processing stage and be an all in one solution (an exploration of EM818 might allow to start with this topic)
- the ITE mechanism has not been fully elucidated. It seems clearly a topic where advances in its understanding or its origin would allow devising better strategies to counter its negative effects. The interaction with plasticity (grain boundary type and DSA) is still an open issue that deserves more investigations.

As recalled previously, corrosion control in molten salt is tightly linked with controlling the redox potential of the salt as well as the content of dissolved impurities (Fe, Cr and oxygen being the one identified here as being of importance). It was evidenced that corrosion is by the control of the chemistry of molten salts (redox potential, impurities, oxide content). Regarding the Te grain boundary embrittlement issue, it seems that a control of the activity of Te is also effective but it requires having some Cr dissolved in the salt. This may be a very easy requirement to fulfill with NiWCr alloys since the Cr oxidation is easier with NiWCr alloys than with NiMoCr. There is potentially a way to have a good balance between corrosion resistance and Te IG cracking resistance. Better defined experimental conditions will be crucial in the future to critically assess the behavior of these materials from the corrosion point of view. One can also wish that long term corrosion testing would become feasible in molten salts.

General recommendations about materials for nuclear reactors

We would like to conclude here by some methodological recommendations from the point of view of designing specific materials for the MSFR. The work done in EVOL has been focused on trying to design a material from the mechanical properties and corrosion point of view. This process is clearly an iterative one. The metallurgy of these alloys allows for successive optimization and this process has just started for NiWCr alloys. While we have clearly made progress in the framework of EVOL, it is clear that much remains still to be done in this area especially given the fact that these materials are supposed to be irradiated. The extensive experience on Nickel alloys irradiation in Oak Ridge lead to the identification of the Helium production issue. A strong embrittlement by He segregation at grain boundaries was identified in Hastelloy N that will also be true for NiWCr alloys. Different metallurgical suggestions come immediately to mind to cope with this: chemistry of fine and dispersed carbides (TiC or else) or oxide dispersed based on Y_2O_3 for example. These are potential research options for designing better irradiation resistant materials. We emphasize the critical need to have a close connection between processing and irradiated material characterization. It is clear that this would be a very ambitious program requiring major work to establish both the processing route for such innovative materials and a consistent database of material properties. The potential in Europe to carry out such a program is there. One can think about several facilities, in France notably, to irradiate these types of materials with the relevant irradiation conditions. We are probably at a stage where such research program becomes feasible.

D- TRAINING AND DISSEMINATION ACTIVITIES

The total number of publications, communications and students involving in the project during the all period (3 years) is:

- **62 publications/proceedings**
- **85 communications in international conferences**
- **14 PhD and 14 Master Thesis**

During the project we have organized 6 European meeting (ROSATOM/EURATOM), 3 workshops and a winter school.